# The discretized backstepping method: an application to a general system of $2 \times 2$ linear balance laws

Mathias Dus

# The discretized backstepping method: an application to a general system of $2 \times 2$ linear balance laws

Mathias Dus

2020

## 1 Introduction

### 1.1 Literature review

In the work, we investigate boundary stabilization of a class of linear first-order hyperbolic systems of Partial Differential Equations (PDEs) on a finite space domain $x \in [0,1]$. Such systems are predominant in modeling of traffic flow [2], heat exchangers [25], open channel flow [4, Chapter 1.4] or multiphase flow [9, 13, 10]. The coupling between states traveling in opposite directions, both in-domain and at the boundaries, may induce instability leading to undesirable behaviors. For example, oscillatory two-phase flow regimes occurring on oil and gas production systems directly result, in some cases, from these mechanisms [10]. The dynamics of most of these industrial systems are described by nonlinear transport equations. If we linearize such systems, one obtains a system of the form:

$$\left\{\begin{array}{lcl} \partial_t R + \Lambda_+(x)\partial_x R &=& M_{11}(x)R + M_{12}(x)S \\ \partial_t S - \Lambda_-(x)\partial_x S &=& M_{21}(x)R + M_{22}(x)S \\ R(t,0) &=& u(t) \\ S(t,1) &=& HR(t,1) \end{array}\right. \tag{1}$$

where $R \in \mathbb{R}^{d_1}, S \in \mathbb{R}^{d_2}$, $\Lambda_+, \Lambda_- > 0$ are positive diagonal matrices and $H, M_{11}, M_{12}, M_{21}, M_{22}$ are matrices of appropriate dimensions. To stabilize system (1), feedback controls $u(t)$ depending on the boundary values $S(t,0)$ were designed. Lyapunov techniques allows to establish exponential stabilization in Sobolev or $C^p$ spaces when the terms $M_{\bullet\bullet}$ are supposed to be small. Applications to Saint Venant systems are given in [15, 16, 8, 5, 12].

However when the in-domain coupling term $M_{\bullet\bullet}$ is too large, a simple quadratic Lyapunov function does not exist [3, 15]. Moreover, spectral analysis shows that when $M_{\bullet\bullet}$ exceed a certain amplitude, the system is unstable for any control of the form $u(t) = FS(t,0)$ ($F \in M_{d_1 d_2}(\mathbb{R})$) [4, Proposition 5.2]. Note that in [4, Proposition 5.2] this was proven only for $d_1 = d_2 = 1$.

To solve this problem, one can relax the assumption of a feedback control depending only on boundary terms and use a full-state feedback control of the form $u(t) = \int_0^1 \alpha(\xi)R(t,\xi) + \beta(\xi)S(t,\xi)d\xi$ ($\alpha(\xi), \beta(\xi)$ are functions taking their values in $[0,1]$). Here, we focus on backstepping controls which is a particular case of full-state feedback controls. Besides, backstepping techniques were primarily designed for ODEs [19] where the main idea is to find a bijective transformation that maps the system in a simpler to stabilize one. There is a vast literature on the extension of backstepping to parabolic and hyperbolic PDEs [24, 20, 23]. The book [21] is a very pedagogical introduction to the topic.

In this paper, we focus on the particular case where $d_1 = d_2 = 1$ that is to say that we have only two heterodirectional transport equations. By a change of variable (see [4, p 176]), it is possible to suppress diagonal zeroth order terms to obtain:

$$\begin{cases} \partial_t R + \lambda_+(x)\partial_x R &= \tilde{M}_{12}(x) S \\ \partial_t S - \lambda_-(x)\partial_x S &= \tilde{M}_{21}(x) R \\ R(t,0) &= u(t) \\ S(t,1) &= hR(t,1) \end{cases}$$

where $h \in \mathbb{R}, \lambda_+, \lambda_- > 0, \tilde{M}_{12}, \tilde{M}_{21} : [0,1] \to \mathbb{R}$, $u(t)$ is the control and $x \in [0,1]$. In this article, we neglect the space dependence of $\lambda_1, \lambda_2, \tilde{M}_{12}, \tilde{M}_{21}$ and suppose that they are constant. Moreover, in order to ease the reading, the tilda notation of $\tilde{M}_{12}, \tilde{M}_{21}$ is dropped in the rest of the paper. As a consequence, the system under consideration writes:

$$\begin{cases} \partial_t R + \lambda_+ \partial_x R &= M_{12} S \\ \partial_t S - \lambda_- \partial_x S &= M_{21} R \\ R(t,0) &= u(t) \\ S(t,1) &= hR(t,1) \end{cases} \tag{2}$$

where $\lambda_+, \lambda_- > 0$ and $M_{12}, M_{21} \in \mathbb{R}$.

More precisely, the focus is on the finite-time stabilization of the system with optimal time in $L^p([0,1])$ $(1 < p \leq \infty)$. The problem is to find a full-state feedback control $u(t)$ such that:

$$\forall t \geq T_{\min} := \frac{1}{\lambda_+} + \frac{1}{\lambda_-}, \ \|R(t,\cdot)\|_{L^p([0,1])} + \|S(t,\cdot)\|_{L^p([0,1])} = 0.$$

In the continuous setting, this problem is already solved [4, Chapter 7.4]. However to the author's knowledge, no result is known when one discretizes the equations. In [1, Section 3.3], the author designs a backstepping control from the continuous theory and inject it in the discretized closed loop. More precisely, inspired from [18], the author uses an iterative algorithm where the characteristic lines are calculated in order to compute the backstepping kernel (see Section 1.2 for the definition of the kernel). However, finding the characteristic lines makes the implementation quite difficult when characteristic velocities are not constant. Here, we do not use the iterative algorithm from [1, Section 3.3], the method rather relies on a finite volume scheme presented in Section 3, that is easier to implement.

To simulate the closed loop system, a classic upwind finite volume scheme is given. With an example, we will see that the finite volume scheme used to compute the backstepping control cannot be chosen arbitrarily. It is mandatory to apply the backstepping method directly on the scheme in itself in order to build a control. More precisely, if the schemes are not wisely chosen, then instabilities occur when the in-domain coupling is large. The contribution can be summed up as follows:

- We illustrate on an example that injecting a control synthesized from an arbitrary finite volume scheme does not stabilize the discretized closed loop system.
- We give a numerical framework for the numerical backstepping theory.
- We prove a finite time stabilization result for the discretized system.

**Outline:** The article is organized as follows. In Section 1.2, we recall the way to compute the backstepping control in the continuous theory. In Section 2, an example is given to show that both schemes for calculating the control and the solution must be wisely chosen. In Section 3, we propose another scheme and prove the finite time stabilization of the numerical system using new discretized backstepping techniques. In Section 4, numerical illustrations of our results are given. Finally, conclusions and perspectives are proposed in the last part of this paper.

## 1.2 The continuous backstepping method

In this section, we recall the continuous backstepping procedure without giving any proof. The system (2) without boundary condition can be rewritten in the form,

$$\partial_t U + \Lambda \partial_x U = MU$$

where

$$U(t,x) = \begin{pmatrix} R(t,x) \\ S(t,x) \end{pmatrix}, \Lambda = \begin{pmatrix} \lambda_+ & 0 \\ 0 & -\lambda_- \end{pmatrix}, M = \begin{pmatrix} 0 & M_{12} \\ M_{21} & 0 \end{pmatrix}.$$

To find a feedback control, we use the strategy of backstepping. A second order Volterra transform allows to pass from the original system (2) to a target system for which finite time extinction is straightforward:

$$\begin{cases} \partial_t U^\star + \Lambda \partial_x U^\star = & 0, \\ U_1^\star(t,0) = & 0, \\ U_2^\star(t,1) = & hU_1^\star(t,1). \end{cases} \tag{3}$$

Note that we got rid of the 0th order term and that after a time $t = T_{\min}$, the solution to (3) is zero for any initial data.

More precisely, the Volterra transform is expressed as follows:

$$U^\star(t,x) = U(t,x) - \int_x^1 P(x,\xi) U(t,\xi) d\xi \tag{4}$$

where $P$ takes its values in $M_{2,2}(\mathbb{R})$ and is defined on the triangle $\{(x,\xi) \mid 0 \leq x \leq \xi \leq 1\}$.

With such transformation, we express the time derivative of $U^\star$:

$$\begin{aligned} \partial_t U^\star(t,x) &= \partial_t U(t,x) - \int_x^1 P(x,\xi) \partial_t U(t,\xi) d\xi \\ &= \partial_t U(t,x) - \int_x^1 P(x,\xi)(-\Lambda \partial_\xi U + MU)(t,\xi) d\xi \\ &= \partial_t U(t,x) + P(x,1)\Lambda U(t,1) - P(x,x)\Lambda U(t,x) \\ &\quad - \int_x^1 (\partial_\xi P \Lambda + PM)(x,\xi) U(t,\xi) d\xi. \end{aligned}$$

For the space derivative:

$$\partial_x U^\star(t,x) = \partial_x U(t,x) + P(x,x)U(t,x) - \textstyle\int_x^1 \partial_x P(x,\xi) U(t,\xi) d\xi.$$

Gathering previous results, one gets the PDE solved by $U^\star$:

$$\begin{aligned} \partial_t U^\star(t,x) + \Lambda \partial_x U^\star(t,x) = & \textstyle\int_x^1 (-\Lambda \partial_x P - \partial_\xi P \Lambda - PM)(x,\xi) U(t,\xi) d\xi \\ & + (M + \Lambda P(x,x) - P(x,x)\Lambda) U(t,x) \\ & + P(x,1)\Lambda U(t,1). \end{aligned}$$

To get that $U^\star$ solves (3), the function $P$ is then chosen as the unique solution to the following system:

$$\begin{cases} \partial_\xi P \Lambda + \Lambda \partial_x P + PM &= 0 \\ M + \Lambda P(x,x) - P(x,x)\Lambda &= 0 \\ P(x,1)\Lambda(1,h)^T &= 0 \end{cases} \tag{5}$$

which is a well-posed transport system. See [4, chapter 7] or [7] for details. This can be rewritten in the usual PDE form as follows:

$$\left\{\begin{array}{rcl}\lambda_+\partial_\xi P_{11}+\lambda_+\partial_x P_{11}= & M_{21}P_{12}\\ \lambda_-\partial_\xi P_{12}-\lambda_+\partial_x P_{12}= & -M_{12}P_{11}\\ \lambda_+\partial_\xi P_{21}-\lambda_-\partial_x P_{21}= & M_{21}P_{22}\\ \lambda_-\partial_\xi P_{22}+\lambda_-\partial_x P_{22}= & -M_{12}P_{21}\end{array}\right. \tag{6}$$

with boundary conditions:

$$\left\{\begin{array}{rcl}P_{12}(x,x) & = & -\frac{M_{12}}{\lambda_++\lambda_-}\\ P_{21}(x,x) & = & \frac{M_{21}}{\lambda_++\lambda_-}\\ P_{11}(x,1) & = & \frac{h\lambda_-}{\lambda_+}P_{12}(x,1)\\ P_{22}(x,1) & = & \frac{\lambda_+}{h\lambda_-}P_{21}(x,1).\end{array}\right. \tag{7}$$

Additionally, let us compute the trace of $U^\star$:

$$\left\{\begin{array}{rcl}U_1^\star(t,0) & = & u(t)-\displaystyle\int_0^1 p_{11}(0,\xi)U_1(t,\xi)+p_{12}(0,\xi)U_2(t,\xi)d\xi\\ U_2^\star(t,1) & = & U_2(t,1)=hU_1(t,1).\end{array}\right.$$

Hence to get the same boundary condition at $x=0$ as in (3), the control $u(t)$ is chosen such that:

$$u(t):=\int_0^1 p_{11}(0,\xi)U_1(t,\xi)+p_{12}(0,\xi)U_2(t,\xi)d\xi. \tag{8}$$

Equations (6)-(8) defines the backstepping control allowing finite-time stabilization for the system under study.

# 2 The numerical backstepping approach: the naive way

In this section, a scheme is proposed to compute the backstepping kernel. It is shown by numerical illustrations that the associated control may not stabilize the closed loop system. This is why, the method is called the "naive" method in contrast with the one presented in Section 3 for which stability will be proved.

## 2.1 The scheme for the closed-loop system

We discretize the state $(R,S)$ introducing two discretization parameters $dt>0, dx=1/N (N\in\mathbb{N})$. The numerical approximation of $R,S$ is piecewise constant on cells $[ndt,(n+1)dt]\times[(j-1)dx,jdx]$ $(n\in\mathbb{N}^\star, 1\le j\le N)$. To designate its values on such cells, we introduce the sequences $(R_j^n,S_j^n)_{n\in\mathbb{N}^\star,1\le j\le N-1}$ and the numerical closed loop system is:

$$\forall j: 1\le j\le N,\ \left\{\begin{array}{rcl}\dfrac{R_j^{n+1}-R_j^n}{dt}+\lambda_+\dfrac{R_j^n-R_{j-1}^n}{dx}= & M_{12}S_j^n\\ \dfrac{S_j^{n+1}-S_j^n}{dt}-\lambda_-\dfrac{S_{j+1}^n-S_j^n}{dx}= & M_{21}R_j^n.\end{array}\right.$$

For boundary conditions, we impose the ghost cell condition:

$$\left\{\begin{array}{rcl}R_0^n= & u^n\\ S_{N+1}^n= & hR_N^{n-1}.\end{array}\right.$$

where $u^n$ is given by:

$$u^n := \sum_{j=1}^{N} (P_{11,N,j} R_j^{n-1} + P_{12,N,j} S_j^{n-1}) dx. \tag{9}$$

where $P_{11}, P_{12}, P_{21}, P_{22} \in M_{N,N}(\mathbb{R})$ are the discretized version of $P$ that will be defined just after.

## 2.2 Resolution of (5)

Before going into the simulations, we need to compute $P$ solving (5) using a scheme that will be chosen later.

Equations in (5) can be seen as as a system of coupled transport equations on a triangular domain drawn in Figure 1:

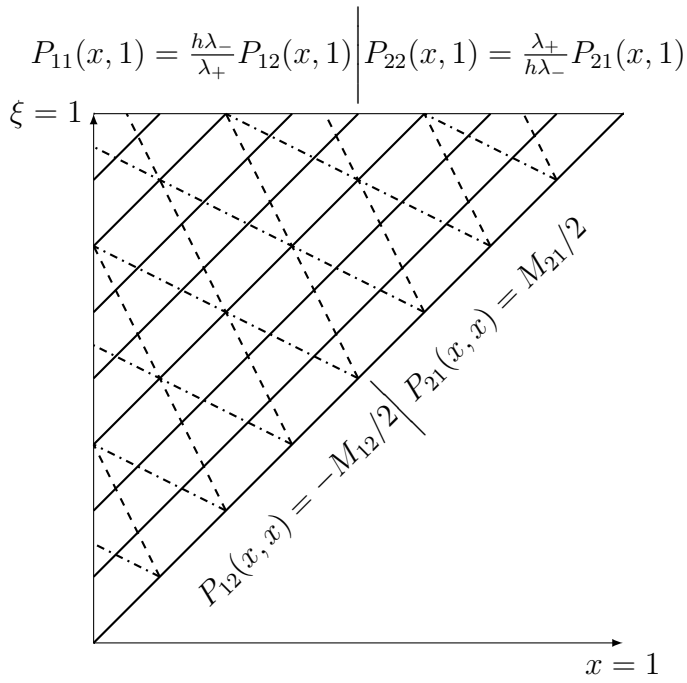


Figure 1: The domain where $P$ is defined

Here, the dot-dashed lines corresponds to characteristics for $P_{12}$ and the dashed ones to those of $P_{21}$ while the plain ones correspond to $P_{11}$ and $P_{22}$.

One can see the variable $x$ as a "time" variable and $\xi$ as a space variable. Boundary conditions are imposed on the diagonal and the upper edge of the triangle. The corresponding "initial data" condition corresponds to the upper right corner of the triangle in Figure 1. In the next section, we give a naive method to solve these transport equations on such triangular domain.

## 2.3 A naive scheme to solve (5)

To solve system (5), a finite difference method is used where $x$ is seen as the time variable while $\xi$ corresponds to the space variable. To do so, we introduce the step $dx = 1/N$ ($N \in \mathbb{N}^*$) and the step $d\xi = 1/N$. The $(x, \xi)$ mesh is then defined by:

$$\forall i \in \mathbb{N}, \quad 1 \leq i \leq N, \quad \left\{ \begin{array}{rcl} x_i & := & (i - 1/2)dx \\ \xi_j & := & (j - 1/2)d\xi. \end{array} \right. \\ i \leq j \leq N$$

As a consequence, the grid is Cartesian (and square) and drawn in Figure 2:

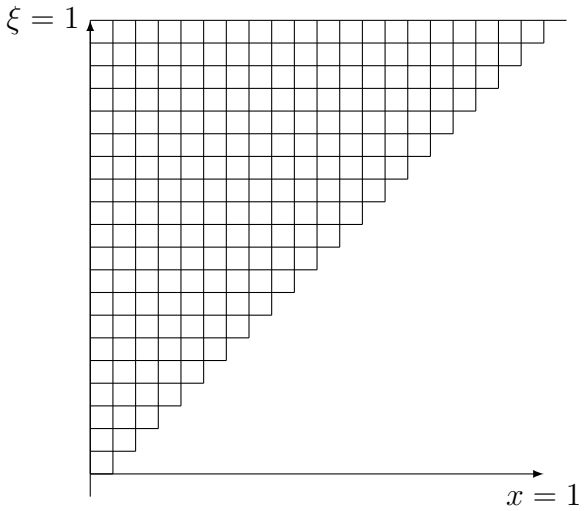


Figure 2: The grid for the computation of $P$

The numerical approximation $P_{i,j}$ of $P$ is piecewise constant on cells of the form $(x_i - dx/2, x_i + dx/2) \times (\xi_j - d\xi/2, \xi_j + d\xi/2)$. It is computed as follows:

- For all $1 \leq j \leq N$, $P_{12,N,j} = -\frac{M_{12}}{\lambda_+ + \lambda_-}$, $P_{21,N,j} = \frac{M_{21}}{\lambda_+ + \lambda_-}$ and $P_{11,N,N} = -\frac{h\lambda_-}{\lambda_+}\frac{M_{12}}{\lambda_+ + \lambda_-}$, $P_{22,N,N} = \frac{\lambda_+}{h\lambda_-}\frac{M_{21}}{\lambda_+ + \lambda_-}$.
- Suppose that $P_{i,\bullet}$ is given for some $i \leq N$. Recalling (6), we calculate to calculate $P_{i-1}$ using an upwind scheme:

$$\begin{array}{lll} \forall j \leq i-1 & P_{12,i-1,j} = & -\frac{M_{12}}{\lambda_+ + \lambda_-} \\ \forall j \geq i & P_{12,i-1,j} = & P_{12,i,j} + \frac{\lambda_- dx}{\lambda_+ d\xi}(P_{12,i,j-1} - P_{12,i,j}) + dx\frac{M_{12}}{\lambda_+}P_{11,i,j}. \end{array}$$

$$\begin{array}{lll} \forall j \leq i-1 & P_{21,i-1,j} = & \frac{M_{21}}{\lambda_+ + \lambda_-} \\ \forall j \geq i & P_{21,i-1,j} = & P_{21,i,j} + \frac{\lambda_+ dx}{\lambda_- d\xi}(P_{21,i,j-1} - P_{21,i,j}) - dx\frac{M_{21}}{\lambda_-}P_{22,i,j}. \end{array}$$

$$\begin{array}{lll} & P_{11,i-1,N} = & \frac{h\lambda_-}{\lambda_+}P_{12,i+1,N} \\ \forall i-1 \leq j < N & P_{11,i-1,j} = & P_{11,i,j} + dx/d\xi(P_{11,i,j+1} - P_{11,i,j}) + dx\frac{M_{21}}{\lambda_+}P_{12,i,j}. \end{array}$$

$$\begin{array}{lll} & P_{22,i-1,N} = & \frac{\lambda_+}{h\lambda_-}P_{21,i+1,N} \\ \forall i-1 \leq j < N & P_{22,i-1,j} = & P_{22,i,j} + dx/d\xi(P_{22,i,j+1} - P_{22,i,j}) - dx\frac{M_{12}}{\lambda_-}P_{21,i,j}. \end{array}$$

- When all lines of $P$ are computed, it is important to impose:

$$\forall i, \forall j < i, \star \in \{11, 12, 21, 22\},\ P_{\star,i,j} = 0$$

to have an upper triangular structure.

**Remark 1.** Note that the scheme for $P_{12}$ exhibits a CFL number equal to $\frac{\lambda_- dx}{\lambda_+ d\xi} = \frac{\lambda_-}{\lambda_+}$ whereas for the scheme for $P_{21}$, the CFL number is $\frac{\lambda_+}{\lambda_-}$. As a consequence, this naive scheme for $P$ is stable only if $\lambda_+ = \lambda_-$. ∘

## 2.4 Numerical experiments

For numerical experiments, we consider three tests illustrating why such a scheme is not appropriate to get a finite time stabilization. In the three cases, we consider the same initial data:

$$\begin{cases} R_j^0 = & -4\sin(50\frac{j}{N}) \\ S_j^0 = & 2\times \mathbb{1}_{\frac{j}{N}<0.5} - \cos(50\frac{j}{N}). \end{cases}$$

1. For $M_{12}=2, M_{21}=-2$, $dt=0.002$, $\lambda_+=\lambda_-=1$ ($T_{\min}=2$), $dx=d\xi=0.0022$ ($N=450$), the energy dynamics is shown in Figure 3:

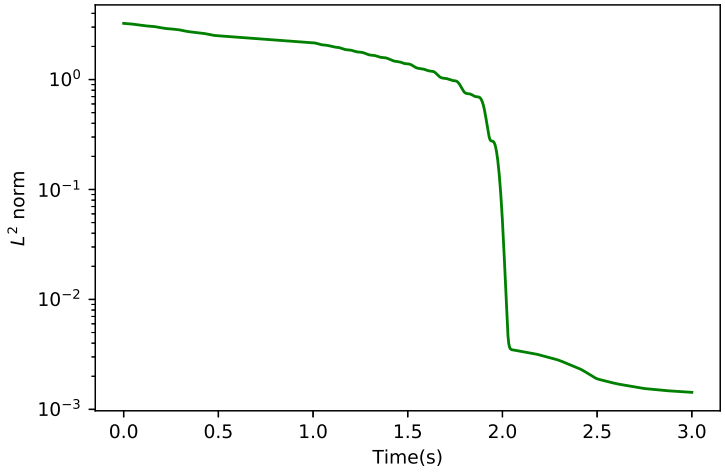


Figure 3: The $L^2$ norm of the solution for case 1

The spectra of the closed-loop and open-loop operators are displayed in Figure 4:

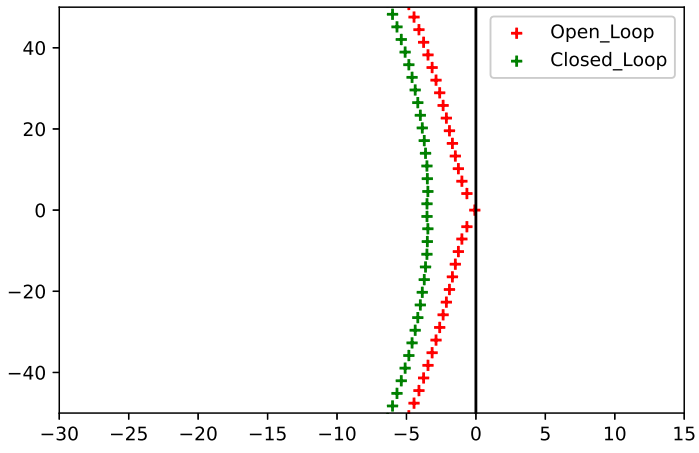


Figure 4: Spectrums of discretized operators for case 1

Here the action of the control is quite satisfying since in Figure 3, one can clearly see that just after the extinction time $T_{\min}$, there is an abrupt decrease of the solution's energy. From a spectral point of view, finite time stabilization is less clear since we have modes of real part around $-4$ which gives an exponential stability with rate equal to $-4$ only.

2. In fact when the coupling term $M$ is too large, it is possible to exhibit the lack of effectiveness of the control synthesized in the previous section. As an example, if we take $M_{12} = 8, M_{21} = -8$ keeping the same discretization parameters $(dt, dx...)$, we obtain Figure 5:

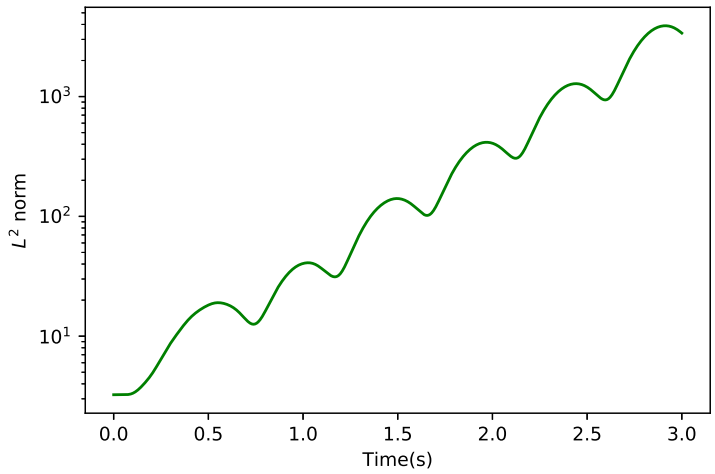


Figure 5: The $L^2$ norm of the solution for case 2

In that case, the spectrum of the closed-loop and open-loop operators are shown in Figure 6:

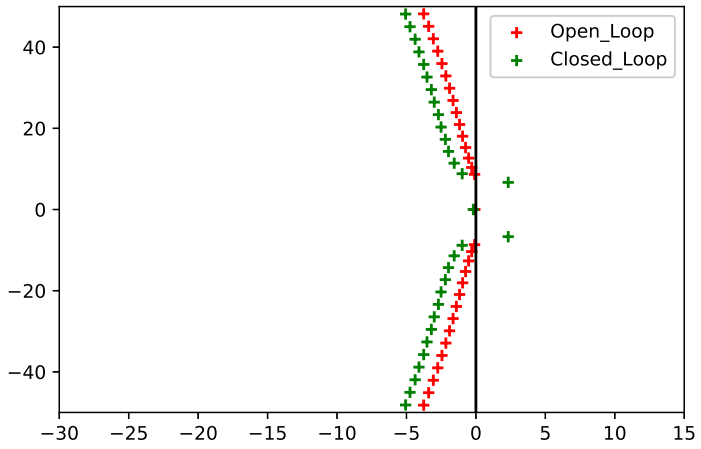


Figure 6: Spectra of discretized operators for case 2

One clearly sees that the closed-loop system is unstable even if the "continuous" (*ie* without discretization) version is finite-time stable.

There is a more efficient way to compute the backstepping control and this is the object of the next section.

# 3 The numerical backstepping approach

In all this section, an initial data $(R^0, S^0)$ is taken in $(L^\infty([0,1]))^2$. In order to remedy the problem of effectiveness of the control highlighted in case 2, we apply directly the Backstepping method on the discretized open-loop system. In addition, we consider two different grids for $R$ and $S$ to avoid problems of CFL pinpointed in Remark 1.

## 3.1 The scheme

Let $N, \alpha$ be integers. In this section, we consider two different space grids (see Figure 7), a coarse grid with $N$ cells, and a fine grid obtained by dividing each coarse cell into $\alpha$ finer cells. Using the notation $dx_+ := \frac{1}{\alpha N}, dx_- := \frac{1}{N}$ and introducing the time step $dt > 0$, one defines the space-time grid by:

$$\left\{\begin{array}{rl} \forall 1 \leq i_c \leq N, & x^c_{i_c} := (i_c - 1/2)dx_- \\ \forall 1 \leq i_f \leq \alpha N, & x^f_{i_f} := (i_f - 1/2)dx_+ \\ \forall n \geq 0, & t^n := ndt. \end{array}\right.$$

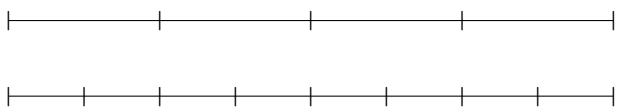

Figure 7: The space grids for $\alpha = 2$

Moreover, the time step $dt > 0$ is given such that the following $CFL$ conditions are satisfied:

$$\left\{\begin{array}{rl} \nu_+ := & \frac{\lambda_+ dt}{dx_+} \leq 1, \\ \nu_- := & \frac{\lambda_- dt}{dx_-} \leq 1. \end{array}\right. \tag{10}$$

The following definition will be useful to pass from the coarse grid to the the finer one and vice-versa.

**Definition 1.** *For all* $1 \leq i_c \leq N$,

$$N_f(i_c) := \left\{1 \leq i_f \leq \alpha N \mid x^f_{i_f} \in [x^c_{i_c} - dx_-/2, x^c_{i_c} + dx_-/2]\right\}.$$

*Moreover,* $1 \leq N_c(i_f) \leq N$ *is the unique index such that* $[x^f_{i_f} - dx_+/2, x^f_{i_f} + dx_+/2] \subset [x_{N_c(i_f)} - dx_-/2, x_{N_c(i_f)} + dx_-/2]$.

The numerical approximation $(R^n)_n \in (\mathbb{R}^{\alpha N})^{\mathbb{N}}$ is piecewise constant on cells of the form $]x^f_{i_f} - dx_+/2, x^f_{i_f} + dx_+/2[$ whereas $(S^n)_n \in (\mathbb{R}^N)^{\mathbb{N}}$ is piecewise constant on cells $]x^c_{i_c} - dx_-/2, x^c_{i_c} + dx_-/2[$. It is computed as follows:

- The initial data is given by $R^0_i = \dfrac{1}{dx_+} \displaystyle\int_{x^f_{i_f} - dx_+/2}^{x^f_{i_f} + dx_+/2} R^0(x)dx$ and $S^0_i = \dfrac{1}{dx_-} \displaystyle\int_{x^c_{i_c} - dx_-/2}^{x^c_{i_c} + dx_-/2} S^0(x)dx$.

- If we assume that $(R^n, S^n)$ is given at time $t^n$, we compute $(R^{n+1}, S^{n+1})$ with:

$$\left\{ \begin{array}{rcl} R^{n+1} & = & R^n + dt(-\lambda_+ \partial_x^+ R^n + M_{12}\Pi_{f\leftarrow c} S^n + Bu^n) \\ S^{n+1} & = & S^n + dt(\lambda_- \partial_x^- S^n + M_{21}\Pi_{c\leftarrow f} R^n + B_2 R^n) \end{array} \right. \tag{11}$$

where operators are defined below.

(i) The positive transport operator $\partial_x^+ \in M_{\alpha N,\alpha N}(\mathbb{R})$ is:

$$\partial_x^+ := \begin{pmatrix} 1/dx_+ & 0 & \cdots & \cdots & 0 \\ -1/dx_+ & 1/dx_+ & \cdots & \cdots & \vdots \\ 0 & -1/dx_+ & 1/dx_+ & \cdots & \vdots \\ \vdots & \cdots & \cdots & \ddots & \vdots \\ 0 & \cdots & \cdots & -1/dx_+ & 1/dx_+ \end{pmatrix},$$

whereas the negative one $\partial_x^- \in M_{N,N}(\mathbb{R})$ is:

$$\partial_x^- := \begin{pmatrix} -1/dx_- & 1/dx_- & \cdots & \cdots & 0 \\ 0 & -1/dx_- & 1/dx_- & \cdots & \vdots \\ 0 & 0 & -1/dx_- & 1/dx_- & \vdots \\ \vdots & \cdots & \cdots & \ddots & \vdots \\ 0 & \cdots & \cdots & 0 & -1/dx_- \end{pmatrix}.$$

(ii) The projection from the coarse grid towards the fine one $\Pi_{f\leftarrow c} \in M_{\alpha N,N}(\mathbb{R})$ is introduced here. To define its action, we take a coarse cell indexed by $1 \leq i_c \leq N$ and a coarse vector $S \in \mathbb{R}^N$:

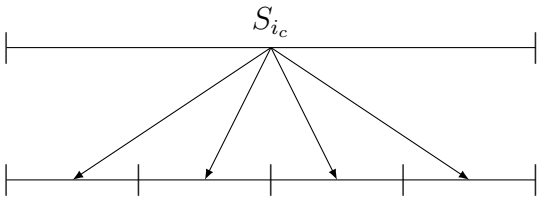


Figure 8: The definition of $\Pi_{f\leftarrow c}$

The fine vector $\Pi_{f\leftarrow c} S \in \mathbb{R}^{\alpha N}$ is constructed by copying the value of $S$ in the coarse cell into the associated fine cells *ie*:

$$\forall j_f \in N_f(i_c), (\Pi_{f\leftarrow c} S)_{j_f} = S_{i_c}.$$

For the projection from the fine grid towards the coarse one, the operator $\Pi_{c\leftarrow f} \in M_{N,\alpha N}(\mathbb{R})$ is constructed here. To define its action, we take a fine vector $R$ and a coarse cell indexed by $1 \leq i_c \leq N$

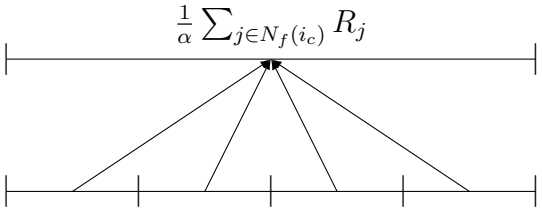


Figure 9: The definition of $\Pi_{c\leftarrow f}$

The coarse value $(\Pi_{c\leftarrow f}R)_{i_c}$ is computed using the arithmetic mean of the values of $R$ in the fine cells corresponding to the neighborhood of the coarse cell $i_c$. Obviously, we have the following dual property:

$$\langle R, \Pi_{f\leftarrow c}S\rangle_f dx_- = \langle \Pi_{c\leftarrow f}R, S\rangle_c dx_+ \tag{12}$$

where $\langle\cdot,\cdot\rangle_f, \langle\cdot,\cdot\rangle_c$ are the respective canonical scalar products in $\mathbb{R}^{\alpha N}, \mathbb{R}^N$.

At a matrix level, this is equivalent to:

$$\Pi_{f\leftarrow c} = \alpha\Pi_{c\leftarrow f}^T. \tag{13}$$

(iii) The discretized boundary control operator $B \in \mathbb{R}^{\alpha N}$ is given below:

$$B := \begin{pmatrix} \lambda_+/dx_+ \\ 0 \\ \vdots \\ 0 \end{pmatrix}.$$

(iv) The boundary transfer operator $B_2 \in M_{N,\alpha N}(\mathbb{R})$ is given by:

$$B_{2,N,\alpha N} := \frac{h\lambda_-}{dx_-}$$

and all other coefficients of $B_2$ are set to zero.

## 3.2 The numerical backstepping method

We apply the backstepping method to the discretized system (11). We look for a backstepping transformation $\mathcal{T}$ as a Volterra transform of the second kind, of the following form:

$$\begin{pmatrix} R^\star \\ S^\star \end{pmatrix} = \mathcal{T}\begin{pmatrix} R \\ S \end{pmatrix} \iff \left\{ \begin{array}{rcl} R^\star &=& R - P_{11}Rdx_+ - P_{12}Sdx_- \\ S^\star &=& S \end{array} \right.$$

The structure of $P_{11}, P_{12}$ is upper triangular in a sense that will be defined later.

The system verified by $R^{\star,n} := R^n - P_{11}R^n dx_+ - P_{12}S^n dx_-$ is calculated below:

$$\begin{array}{rl} \dfrac{R^{\star n+1} - R^{\star n}}{dt} = & \dfrac{R^{n+1}-R^n}{dt} - P_{11}(-\lambda_+\partial_x^+ R^n + M_{12}\Pi_{f\leftarrow c}S^n + Bu^n)dx_+ \\ & -P_{12}(\lambda_-\partial_x^- S^n + M_{21}\Pi_{c\leftarrow f}R^n + B_2R^n)dx_- \end{array}$$

Moreover,

$$\lambda_+\partial_x^+ R^{\star n} = \lambda_+\partial_x^+ R^n - \lambda_+\partial_x^+(P_{11}R^n dx_+ + P_{12}S^n dx_-).$$

Thus, the equation for $R^\star$ reads:

$$\begin{array}{rcl}\dfrac{R^{\star n+1}-R^{\star n}}{dt} + \lambda_+\partial_x^+ R^{\star n} &=& M_{12}\Pi_{f\leftarrow c}S^n + Bu^n - \lambda_+\partial_x^+(P_{11}R^n dx_+ + P_{12}S^n dx_-)\\ && -P_{11}(-\lambda_+\partial_x^+ R^n + M_{12}\Pi_{f\leftarrow c}S^n + Bu^n)dx_+\\ && -P_{12}(\lambda_-\partial_x^- S^n + M_{21}\Pi_{c\leftarrow f}R^n + B_2R^n)dx_-\\ &=& -\Gamma_{11}R^n - \Gamma_{12}S^n + (B - P_{11}Bdx_+)u^n,\end{array} \tag{14}$$

where the terms $\Gamma_{11}, \Gamma_{12}$ are given below:

$$\begin{array}{rcl}\Gamma_{11} &:=& \lambda_+\partial_x^+ P_{11}dx_+ - \lambda_+ P_{11}\partial_x^+ dx_+ + P_{12}(M_{21}\Pi_{c\leftarrow f} + B_2)dx_-,\\ \Gamma_{12} &:=& \lambda_+\partial_x^+ P_{12}dx_- + \lambda_- P_{12}\partial_x^- dx_- + M_{12}P_{11}\Pi_{f\leftarrow c}dx_+ - M_{12}\Pi_{f\leftarrow c}.\end{array} \tag{15}$$

In what follows, we give a scheme that construct a $P$ such that most of the terms of $\Gamma$ are equal to zero. To do so, we see the column index of $P$ (the "$x$" variable) as a time variable whereas row's index is seen as the space variable (the "$\xi$" variable). The scheme is given below:

- We begin by setting the last lines of $P_{11}, P_{12}$:

$$\begin{array}{ll}\forall 1 \le j_f \le \alpha N, & P_{11,\alpha N, j_f} = 0\\ \forall 1 \le j_c \le N, & P_{12,\alpha N, j_c} = 0\end{array} \tag{16}$$

- Suppose that $P_{12}, P_{11}$ is given at rows $i_f, \cdots, \alpha N$, then we calculate $P_{12,i_f-1,j_c}$ by imposing $\Gamma_{12,i_f,j_c} = 0$ for $j_c \ge N_c(i_f - 1)$. From (15), we deduce:

$$\lambda_+\frac{P_{12,i_f,j_c} - P_{12,i_f-1,j_c}}{dx_+}dx_- - \lambda_-\frac{P_{12,i_f,j_c} - P_{12,i_f,j_c-1}}{dx_-}dx_- + M_{12}[P_{11}\Pi_{f\leftarrow c}]_{i_f,j_c}dx_+ - M_{12}[\Pi_{f\leftarrow c}]_{i_f,j_c} = 0. \tag{17}$$

It is easy to compute $[P_{11}\Pi_{f\leftarrow c}]_{i_f,j_c}$ using local indexes. Using (13), one gets:

$$[P_{11}\Pi_{f\leftarrow c}]_{i_f,j_c} = [\Pi^T_{f\leftarrow c}P^T_{11}]_{j_c,i_f} = \alpha[\Pi_{c\leftarrow f}P^T_{11}]_{j_c,i_f} = \sum_{i\in N_f(j_c)} P_{11,i_f,i}.$$

Then, we compute $P_{11,i_f-1,j_f}$ imposing $\Gamma_{11,i_f,j_f} = 0$ for $j_f \ge i_f - 1$:

$$\lambda_+\frac{P_{11,i_f,j_f} - P_{11,i_f-1,j_f}}{dx_+}dx_+ - \lambda_+\frac{P_{11,i_f,j_f} - P_{11,i_f,j_f+1}}{dx_+}dx_+ + M_{21}[P_{12}\Pi_{c\leftarrow f}]_{i_f,j_f}dx_- + [P_{12}B_2]_{i_f,j_f}dx_- = 0. \tag{18}$$

It is easy to calculate $[P_{12}\Pi_{c\leftarrow f}]_{i_f,j_f}$ using local indexes. Using (13), one obtains:

$$[P_{12}\Pi_{c\leftarrow f}]_{i_f,j_f} = [\Pi^T_{c\leftarrow f}P^T_{12}]_{j_f,i_f} = \frac{1}{\alpha}[\Pi_{f\leftarrow c}P^T_{12}]_{j_f,i_f} = \frac{1}{\alpha}P_{12,i_f,N_c(j_f)}.$$

For $[P_{12}B_2]_{i_f,j_f}$, we also have:

$$[P_{12}B_2]_{i_f,j_f} = \frac{h\lambda_-}{dx_-}P_{12,i_f,N}\delta_{j_f=\alpha N}.$$

**Algorithm 1** Calculate $P_{12}$

$P_{12,i_f,j_c} \leftarrow 0$ for all $1 \leq i_f \leq \alpha N, 1 \leq j_c \leq N$.
**for** $2 \leq i_f \leq \alpha N$ (step = -1) **do**
  **for** $N_c(i_f - 1) \leq j_c \leq N$ **do**
    **if** $j_c = N_c(i_f)$ **then**
      $P_{12,i_f-1,j_c} \leftarrow -\frac{M_{12}}{\alpha\lambda_+}$
    **end if**
    $P_{12,i_f-1,j_c} \leftarrow P_{12,i_f-1,j_c} + (1 - \frac{\lambda_-}{\lambda_+}\frac{dx_+}{dx_-})P_{12,i_f,j_c} + \frac{\lambda_-}{\lambda_+}\frac{dx_+}{dx_-}P_{12,i_f,j_c-1}$ (transport)
    $P_{12,i_f-1,j_c} \leftarrow P_{12,i_f-1,j_c} + \frac{M_{12}}{\alpha\lambda_+}\sum_{j_f \in N_f(j_c)} P_{11,i_f,j_f}dx_+$ (exchange)
  **end for**
**end for**

**Algorithm 2** Calculate $P_{11}$

$P_{11,i_f,j_f} \leftarrow 0$ for all $1 \leq i_f \leq \alpha N, 1 \leq j_f \leq \alpha N$.
**for** $2 \leq i_f \leq \alpha N$ (step = -1) **do**
  $P_{11,i_f-1,\alpha N} \leftarrow \frac{h\lambda_-}{\lambda_+}P_{12,i_f,N}$
  **for** $i_f - 1 \leq j_f \leq \alpha N$ **do**
    **if** $j_f \neq \alpha N$ **then**
      $P_{11,i_f-1,j_f} \leftarrow P_{11,i_f-1,j_f} + P_{11,i_f,j_f+1}$ (transport)
    **end if**
    $P_{11,i_f-1,j_f} \leftarrow P_{11,i_f-1,j_f} + M_{21}P_{12,i_f,N_c(j_f)}\frac{dx_-}{\alpha\lambda_+}$ (exchange)
  **end for**
**end for**

**Remark 2.** The algorithms immediately give that:

$$\begin{cases} \forall j_f < i_f, & P_{11,i_f,j_f} = 0 \\ \forall j_c < N_c(i_f), & P_{12,i_f,j_c} = 0. \end{cases} \tag{19}$$

∘

## 3.3 Convergence properties of the kernel

In what follows and until the end of the article, $C$ designates a constant independent on the discretization. Here we present a boundedness result for $P$ which will be useful later:

**Proposition 1.** *If* $\frac{\lambda^-}{\lambda^+}\frac{dx_+}{dx_-} \leq 1$, *there exists* $C_\infty > 0$ *independent on* $N$ *such that:*

$$\|P_{11}\|_{L^\infty([0,1]^2)} + \|P_{12}\|_{L^\infty([0,1]^2)} \leq C_\infty. \tag{20}$$

**Remark 3.** The condition:

$$\frac{\lambda^-}{\lambda^+}\frac{dx_+}{dx_-} \leq 1$$

can be interpreted as a CFL condition. It imposes an asymmetry of grids in the sense that if $\frac{\lambda_-}{\lambda_+} > 1$, the grid for $R$ (where the control is applied) needs to be finer than the one for $S$. ∘

*Proof.* The scheme verified by $P_{12}$ gives:

$$\begin{aligned}\forall j_c > N_c(i_f), |P_{12,i_f-1,j_c}| \leq \quad & (1-\tfrac{\lambda_-}{\lambda_+}\tfrac{dx_+}{dx_-})|P_{12,i_f,j_c}| + \tfrac{\lambda_-}{\lambda_+}\tfrac{dx_+}{dx_-}|P_{12,i_f,j_c-1}| \\ & + \frac{|M_{12}|}{\alpha\lambda_+}\sum_{j\in N_f(j_c)}|P_{11,i_f,j}|dx_+. \end{aligned} \tag{21}$$

For $j_c \leq N_c(i_f) - 1$, we have:

$$|P_{12,i_f-1,j_c}| = \quad 0, \tag{22}$$

whereas for $j_c = N_c(i_f)$, it holds:

$$|P_{12,i_f-1,j_c}| \leq \quad \left(1-\frac{\lambda_-}{\lambda_+}\frac{dx_+}{dx_-}\right)|P_{12,i_f,j_c}| + \left|\frac{M_{12}}{\lambda_+\alpha}\right| + \frac{|M_{12}|}{\lambda_+\alpha}\sum_{j\in N_f(j_c)}|P_{11,i_f,j}|dx_+. \tag{23}$$

Combining (21)-(23), it holds:

$$\|P_{12,i_f-1,\cdot}\|_{L^\infty([0,1])} = \quad \max\left\{\|P_{12,i_f,\cdot}\|_{L^\infty([0,1])}, \left|\frac{M_{12}}{\lambda_-}\right|\right\} + C\|P_{11,i_f,\cdot}\|_{L^\infty([0,1])}dx_+.$$

Similarly, it holds:

$$\|P_{11,i_f-1,\cdot}\|_{L^\infty([0,1])} \leq \max\left\{\|P_{11,i_f,\cdot}\|_{L^\infty([0,1])}, \frac{h\lambda_-}{\lambda_+}\|P_{12,i_f,\cdot}\|_{L^\infty([0,1])}\right\} + C\|P_{12,i_f,\cdot}\|_{L^\infty([0,1])}dx_-.$$

Denoting
$A_{i_f} := \max\{\frac{h\lambda_-}{\lambda_+}\|P_{12,i_f,\cdot}\|_{L^\infty([0,1])}, \|P_{11,i_f,\cdot}\|_{L^\infty([0,1])}, \left|\frac{hM_{12}}{\lambda_+}\right|\}$, it holds:

$$A_{i_f-1} \leq (1+Cdx_-)A_{i_f}$$

and hence:

$$\forall 1 \leq i_f \leq \alpha N,\ A_{i_f} \leq e^{i_f C dx_-} \leq e^{C\alpha}.$$

□

Finally, in order to exhibit the exact target system, we need to see which term of $\Gamma$ is zero:

**Lemma 1.** *The matrix $\Gamma_{12}$ is zero except for the first row. Moreover, the term $\Gamma_{11,i_f,j_f}$ is non zero only for $j_f \in [\![i_f - \alpha, i_f - 2]\!]$ and $i_f = 1$. Hence, $\Gamma_{11}$ can be decomposed as $\Gamma_{11} =: \tilde{\Gamma}_{11} + \bar{\Gamma}_{11}$ where $\tilde{\Gamma}_{11}$ is the subdiagonal part of $\Gamma_{11}$ and $\bar{\Gamma}_{11} = \Gamma_{11} - \tilde{\Gamma}_{11}$ is non zero only on its first row. Furthermore,*

$$\sup_{i_f,j_f}|\tilde{\Gamma}_{11,i_f,j_f}| \leq Cdx_-.$$

*with $C > 0$ is independent on the discretization.*

In order to see which entry is zero, we represent $\Gamma_{11}, \Gamma_{12}$ for $\alpha = 3$ putting a cross on each non zero entry in Figures 10-11:

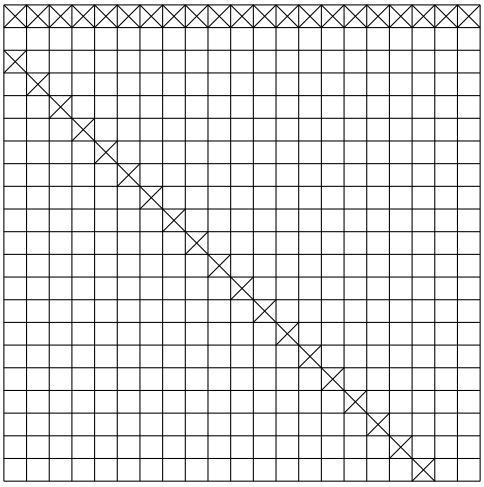

Figure 10: The non zero coefficients for $\Gamma_{11}$ ($\alpha = 3$)

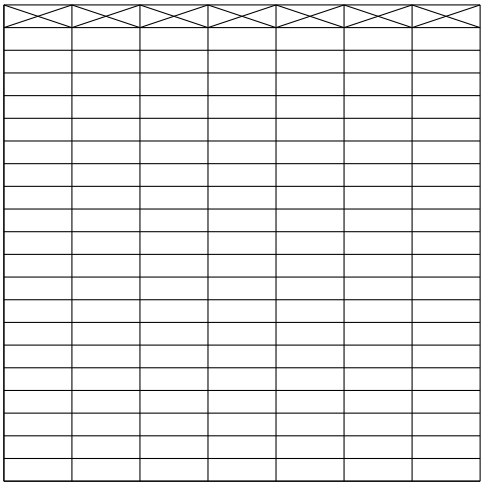

Figure 11: The non zero coefficients for $\Gamma_{12}$ ($\alpha = 3$)

*Proof.* Let $i_f \geq 2$. For $j_c \geq N_c(i_f - 1)$ and by Algorithm 1, we have $\Gamma_{12,i_f,j_c} = 0$. For $j_c \leq N_c(i_f) - 2$, we have:

1. $j_c < N_c(i_f - 1)$ and $P_{12,i_f-1,j_c} = 0$.
2. $j_c < N_c(i_f)$ and $P_{12,i_f,j_c} = 0$.
3. For all $j_f \in N_f(j_c)$, we have $j_f < i_f$ (because $j_c \leq N_c(i_f)-2$ by assumption) and hence $P_{11,i_f,j_f} = 0$.

By the definition of $\Gamma_{12}$, $\Gamma_{12,i_f,j_c} = 0$.

Now for $j_c = N_c(i_f) - 1$, then points 2 and 3 of the previous case hold. If $j_c = N_c(i_f - 1)$, then by Algorithm 1, $\Gamma_{12,i_f,j_c} = 0$. Otherwise, $j_c < N_c(i_f - 1)$ implying that $P_{12,i_f-1,j_c} = 0$. Thus, by the definition of $\Gamma_{12,i_f,j_c}$, one gets $\Gamma_{12,i_f,j_c} = 0$.

For $\Gamma_{11,i_f,j_f}$, the only terms that could be non zero are terms such that $i_f - \alpha + 1 \leq j_f < i_f - 1$ and by the definition of $\Gamma_{11}$:

$$|\Gamma_{11,i_f,j_f}| \leq C\|P_{12}\|_{L^\infty([0,1]^2)}dx_- \leq Cdx_-$$

where we have used Proposition 1.

□

**Remark 4.** If $\alpha \leq 2$ then:

$$\sup_{i_f>1, j_f} |\tilde{\Gamma}_{11,i_f,j_f}| = 0.$$

Indeed, the condition $i_f - \alpha + 1 \leq j_f < i_f - 1 \iff i_f - \alpha + 1 \leq j_f \leq i_f - 2$ is empty.

∘

From the computations of the kernel $P$, we obtained that all the entries of $\Gamma_{11}, \Gamma_{12}$ are zero except for the first row and some diagonal terms in $\Gamma_{11}$. By (14), in order to get rid of the contribution of these first rows, we impose a control $u^n$ of the form:

$$u^n = \frac{1}{\lambda_+ - [P_{11}B]_{11}dx_+^2}\Big(\sum_{j_f=1}^{\alpha N} \Gamma_{11,1,j_f} R^n_{j_f} dx_+ + \sum_{j_c=1}^{N} \Gamma_{12,1,j_c} S^n_{j_c} dx_+\Big) \tag{24}$$

and thus, the final target system is:

$$\left\{\begin{array}{rcl} \dfrac{R^{\star n+1} - R^{\star n}}{dt} + \lambda_+ \partial_x^+ R^{\star n} & = & \tilde{\Gamma}_{11} R^n \\ \dfrac{S^{\star n+1} - S^{\star n}}{dt} - \lambda_- \partial_x^- S^{\star n} & = & B_2 R^n + M_{21}\Pi_{c\leftarrow f} R^n \end{array}\right. \tag{25}$$

where $\tilde{\Gamma}_{11}$ is the subdiagonal part of $\Gamma_{11}$ (see Figure 10).

Next proposition asserts that the discrete Voltera transform of the second kind is invertible and continuous uniformly with respect to the parameter of discretization. This will be useful to express the target system uniquely in terms of star variables. Before presenting the result, it is needed to introduce the $L^p$ $(1 < p < \infty)$ norm for vectors $R \in \mathbb{R}^{\alpha N}, S \in \mathbb{R}^N$:

$$\|R\|_{L^p([0,1])} = \sqrt[p]{\sum_{j_f=1}^{\alpha N} |R_{j_f}|^p dx_+} \text{ and } \|S\|_{L^p([0,1])} = \sqrt[p]{\sum_{j_c=1}^{N} |S_{j_c}|^p dx_-}.$$

**Proposition 2.** *Let $1 < p \leq \infty$. There exists $C > 0$ independent on the discretization such that if $dx_- < C$, then the operator $\mathcal{T}$ is invertible as an operator from $L^p([0,1])$ into $L^p([0,1])$. Moreover, there exists a $C_{back,p} > 0$ independent on the discretization such that for all $R \in \mathbb{R}^{\alpha N}, S \in \mathbb{R}^N$:*

$$\frac{1}{C_{back,p}} \|\mathcal{T}(R,S)\|_{L^p([0,1])} \leq \|(R,S)\|_{L^p([0,1])} \leq C_{back,p} \|\mathcal{T}(R,S)\|_{L^p([0,1])}. \tag{26}$$

*Moreover, there exists $L_{11} \in M_{\alpha N,\alpha N}(\mathbb{R}), L_{12} \in M_{\alpha N,N}(\mathbb{R})$ such that:*

$$\forall R^\star \in \mathbb{R}^{\alpha N}, S^\star \in \mathbb{R}^N,\ \mathcal{T}^{-1}\begin{pmatrix} R^\star \\ S^\star \end{pmatrix} = \begin{pmatrix} R^\star + L_{11}R^\star dx_+ + L_{12}S^\star dx_- \\ S^\star \end{pmatrix}.$$

*where $(L_{11}, L_{12})$ is upper triangular in the sense of* (19).

*Proof.* The first inequality is easy to prove owing Proposition 1 (the proof is left to the reader).

For the second one, we use a fixed point argument. Let $(R^k)_k$ be the sequence such that $R^0 = 0_{\mathbb{R}^{\alpha N}}$ and:

$$\forall k \geq 0,\ R^{k+1} = R^\star + P_{11}R^k dx_+ + P_{12}S^\star dx_-.$$

We estimate $R^{k+1}-R^k$ in a weighted space. More precisely, let $\gamma>0$ and for all $1\leq i_f\leq \alpha N$

$$\begin{aligned}(R^{k+1}_{i_f}-R^k_{i_f})e^{\gamma x^f_{i_f}} &= \sum_{j_f} P_{11,i_f,j_f}(R^k_{j_f}-R^{k-1}_{j_f})e^{\gamma x^f_{i_f}}dx_+\\ &= \sum_{j_f} P_{11,i_f,j_f}e^{-\gamma(x^f_{j_f}-x^f_{i_f})}(R^k_{j_f}-R^{k-1}_{j_f})e^{\gamma x^f_{j_f}}dx_+.\end{aligned}$$

For the case $p=\infty$, we have:

$$\|R^{k+1}-R^k\|_{L^\infty_\gamma([0,1])} \leq \sup_{i_f}\sum_{j_f}|P_{11,i_f,j_f}|e^{-\gamma(x^f_{j_f}-x^f_{i_f})}dx_+\|R^k-R^{k-1}\|_{L^\infty_\gamma([0,1])}. \tag{27}$$

where $L^\infty_\gamma$ is the weighted $L^\infty$ norm:

$$\forall R\in\mathbb{R}^{\alpha N},\ \|R\|_{L^\infty_\gamma([0,1])}:=\max|R_{i_f}|e^{\gamma x^f_{i_f}}.$$

Because of the uniform estimate from Proposition 1 and the upper triangular structure (19), one gets:

$$\begin{aligned}\sup_{i_f}\sum_{j_f}|P_{11,i_f,j_f}|e^{-\gamma(x^f_{j_f}-x^f_{i_f})}dx_+ &\leq C_\infty \sup_{i_f}\sum_{j_f\geq i_f}e^{-\gamma(x^f_{j_f}-x^f_{j_f})}dx_+\\ &= C_\infty\sup_{i_f}\sum_{j_f\geq i_f}e^{-\gamma(x^f_{j_f}-x^f_{i_f})}dx_+\\ &\leq C_\infty\tfrac{dx_+}{1-e^{-\gamma dx_+}}=\tfrac{C_\infty}{\gamma}\tfrac{\gamma dx_+}{1-e^{-\gamma dx_+}}.\end{aligned} \tag{28}$$

Using the boundedness around 0 of the function $x\mapsto\frac{x}{1-e^{-x}}$ and taking $dx_+\leq C/\gamma$:

$$\sup_{i_f}\sum_{j_f}|P_{11,i_f,j_f}|e^{-\gamma(x^f_{j_f}-x^f_{i_f})}dx_+\leq\frac{2C_\infty}{\gamma}.$$

With $4C_\infty\leq\gamma$ and $dx_+\leq C/\gamma$ (with $dx_+<\frac{C}{4C_\infty}$):

$$\forall n>0,\|R^{k+1}-R^k\|_{L^\infty_\gamma([0,1])}\leq\frac{1}{2}\|R^k-R^{k-1}\|_{L^\infty_\gamma([0,1])}.$$

For the case $1<p<\infty$, the conjugate exponent is $q:=\frac{p}{p-1}$ and:

$$\|R^{k+1}-R^k\|_{L^p_\gamma([0,1])}\leq\sqrt[p]{\sum_{i_f}\left(\sum_{j_f}|P_{11,i_f,j_f}|^q e^{-\gamma q(x^f_{j_f}-x^f_{i_f})}dx_+\right)^{\frac{p}{q}}dx_+}\|R^k-R^{k-1}\|_{L^p_\gamma([0,1])}$$

where:

$$\forall R\in\mathbb{R}^{\alpha N},\ \|R\|_{L^p_\gamma([0,1])}:=\sqrt[p]{\sum_{j_f}|R_{j_f}|^p e^{p\gamma x^f_{i_f}}}.$$

Using Proposition 1, (19) and for $dx_+\leq C/\gamma$, we get by similar computations as in (28), that:

$$\sqrt[p]{\sum_{i_f}\left(\sum_{j_f}|P_{11,i_f,j_f}|^q e^{-\gamma q(x^f_{j_f}-x^f_{i_f})}dx_+\right)^{\frac{p}{q}}dx_+}<C_\infty\left(\frac{2}{q}\right)^{1/q}\gamma^{-1/q}$$

and for $\frac{2^{q+1}C^q_\infty}{q}\leq\gamma$ and $dx_+\leq C/\gamma$:

$$\forall n > 0, \|R^{k+1} - R^k\|_{L^p_\gamma([0,1])} \leq \frac{1}{2}\|R^n - R^{k-1}\|_{L^p_\gamma([0,1])}.$$

As a consequence, for $1 < p \leq \infty$ the series $\sum_{k=0}^{\infty} R^{k+1} - R^k$ is convergent and the sequence $(R^k)_k$ converges in $L^p([0,1])$ towards a limit $R \in L^p([0,1])$. Moreover, we have for $\gamma$ large enough:

$$\begin{aligned}
\|R\|_{L^p_\gamma([0,1])} &\leq \sum_{k=0}^{\infty} \|R^{k+1} - R^k\|_{L^p_\gamma([0,1])} \\
&\leq \left(\sum_{k=0}^{\infty} \frac{1}{2^k}\right) \|R^1\|_{L^p_\gamma([0,1])} \\
&\leq \left(\sum_{k=0}^{\infty} \frac{1}{2^k}\right) (\|R^\star\|_{L^p_\gamma([0,1])} + \|S^\star\|_{L^p_\gamma([0,1])}).
\end{aligned}$$

Using the fact that $\|\cdot\|_{L^p([0,1])} \leq \|\cdot\|_{L^p_\gamma([0,1])} \leq e^\gamma \|\cdot\|_{L^p([0,1])}$, one finally gets:

$$\|R\|_{L^p([0,1])} \leq \left(\sum_{k=0}^{\infty} \frac{1}{2^k}\right) e^\gamma (\|R^\star\|_{L^p([0,1])} + \|S^\star\|_{L^p([0,1])}).$$

This proves (26) taking $\gamma = \frac{2^{q+1} C_\infty^q}{q}$ which does not depend on the discretization.

To finish the proof of the proposition, it suffices to write that:

$$\begin{pmatrix} R \\ S \end{pmatrix} = \begin{pmatrix} R^\star \\ S^\star \end{pmatrix} + \begin{pmatrix} P_{11} dx_+ & P_{12} dx_- \\ 0 & 0 \end{pmatrix} \begin{pmatrix} R \\ S \end{pmatrix}$$

and by induction, it holds:

$$\begin{pmatrix} R \\ S \end{pmatrix} = \begin{pmatrix} R^\star \\ S^\star \end{pmatrix} + \sum_{k=1}^{\infty} \begin{pmatrix} P_{11} dx_+ & P_{12} dx_- \\ 0 & 0 \end{pmatrix}^k \begin{pmatrix} R^\star \\ S^\star \end{pmatrix}.$$

Owing the strict upper triangular structure of $P_{\bullet,\bullet}$, we get that:

$$\begin{pmatrix} L_{11} dx_+ & L_{12} dx_- \\ 0 & 0 \end{pmatrix} := \sum_{k=1}^{\infty} \begin{pmatrix} P_{11} dx_+ & P_{12} dx_- \\ 0 & 0 \end{pmatrix}^k$$

with $L_{11}$ strict upper triangular and $L_{12}$ verifying (19) (easy to prove by induction).

□

## 3.4 Proof of the finite time stabilization result

Owing Proposition 2, it is possible to write the target system (25) as:

$$\left\{ \begin{array}{rcl} \dfrac{R^{\star n+1} - R^{\star n}}{dt} + \lambda_+ \partial_x^+ R^{\star n} &=& \tilde{\Gamma}_{11} R^n \\ \dfrac{S^{\star n+1} - S^{\star n}}{dt} - \lambda_- \partial_x^- S^{\star n} &=& (B_2 + M_{21} \Pi_{c \leftarrow f})(R^{\star n} + L_{11} R^{\star n} dx_+ + L_{12} S^{\star n} dx_-). \end{array} \right. \tag{29}$$

Then using Lemma 1, next lemma shows that the right hand side of the equation for $R^\star$ in (29) can be neglected.

**Lemma 2.** *For all $T > 0$ and $1 < p < \infty$, there exists $C > 0$ independent on the parameters of discretization such that:*

$$\forall n : ndt \leq T, \|R^{\star n} - \tilde{R}^{\star n}\|^p_{L^p([0,1])} + \|S^{\star n} - \tilde{S}^{\star n}\|^p_{L^p([0,1])} \leq C dx_-^p \sum_{m=0}^{n} (\|R^{\star m}\|^p_{L^p([0,1])} + \|S^{\star m}\|^p_{L^p([0,1])}) dt.$$

*where $\tilde{R}^\star, \tilde{S}^\star$ satisfies the same system as (29) without the term $\Gamma_{11}$, that is*

$$\left\{ \begin{array}{rl} \dfrac{\tilde{R}^{\star n+1} - \tilde{R}^{\star n}}{dt} + \lambda_+ \partial_x^+ \tilde{R}^\star_n = & 0 \\ \dfrac{\tilde{S}^{\star n+1} - \tilde{S}^{\star n}}{dt} - \lambda_- \partial_x^- \tilde{S}^{\star n} = & (B_2 + M_{21}\Pi_{c\leftarrow f})(\tilde{R}^{\star n} + L_{11}\tilde{R}^{\star n} dx_+ + L_{12}\tilde{S}^{\star n} dx_-), \end{array} \right. \tag{30}$$

*with initial data:*

$$\left\{ \begin{array}{rl} \tilde{R}^{\star 0} = & R^{\star 0} \\ \tilde{S}^{\star 0} = & S^{\star 0}. \end{array} \right.$$

Before going into the proof of Lemma 2, we will prove the following preliminary result:

**Lemma 3.** *For all $T > 0$, there exists $C > 0$ independent on the discretization such that for every $(f^n)_n \in (\mathbb{R}^{\alpha N})^{\mathbb{N}}$ and every $(\tilde{R}^{\star n}, \tilde{S}^{\star n})_n$ satisfying:*

$$\left\{ \begin{array}{rl} \dfrac{\tilde{R}^{\star n+1} - \tilde{R}^{\star n}}{dt} + \lambda_+ \partial_x^+ \tilde{R}^{\star n} = & f^n \\ \dfrac{\tilde{S}^{\star n+1} - \tilde{S}^{\star n}}{dt} - \lambda_- \partial_x^- \tilde{S}^{\star n} = & (B_2 + M_{21}\Pi_{c\leftarrow f})(\tilde{R}^{\star n} + L_{11}\tilde{R}^{\star n} dx_+ + L_{12}\tilde{S}^{\star n} dx_-), \end{array} \right. \tag{31}$$

*then:*

$$\forall n : ndt \leq T, \|\tilde{R}^{\star n}\|^p_{L^p([0,1])} + \|\tilde{S}^{\star n}\|^p_{L^p([0,1])} \leq C \left( \|\tilde{R}^{\star 0}\|^p_{L^p([0,1])} + \|\tilde{S}^{\star 0}\|^p_{L^p([0,1])} + \sum_{k=0}^{n} \|f^n\|^p_{L^p([0,1])} dt \right).$$

*Proof.* As this is classical, we give only a rapid sketch of the proof here.

Let $1 < p < \infty$, then by the convexity of $x \to |x|^p$:

$$\forall j_f \geq 2,\ |\tilde{R}^{\star n+1}_{j_f}|^p \leq (1+dt)^{p-1}\big((1-\nu_+)|\tilde{R}^{\star n}_{j_f}|^p + \nu_+ |\tilde{R}^{\star n}_{j_f-1}|^p + dt|f^n_{j_f}|^p\big).$$

Hence, summing over $j_f$ and multiplying by $dx_+$, one gets:

$$\|\tilde{R}^{\star n+1}\|^p_{L^p([0,1])} \leq (1+dt)^{p-1}\big(\|\tilde{R}^{\star n}\|^p_{L^p([0,1])} + dt\|f^n\|^p_{L^p([0,1])} - \nu_+ |\tilde{R}^{\star n}_{\alpha N}|^p dx_+\big).$$

For $S^\star$, the method is similar:

$$\begin{array}{rl} \forall j_c \leq N-1,\ |\tilde{S}^{\star n+1}_{j_c}|^p \leq & (1+Cdt)^{p-1}\Big((1-\nu_-)|\tilde{S}^{\star n}_{j_c}|^p + \nu_- |\tilde{S}^{\star n}_{j_c+1}|^p \\ & + dt|M_{21}|\big(|[\Pi_{c\leftarrow f} L_{11}\tilde{R}^{\star n}]_{j_c} dx_+|^p + |[\Pi_{c\leftarrow f} L_{12}\tilde{S}^{\star n}]_{j_c} dx_-|^p \\ & + |[\Pi_{c\leftarrow f}\tilde{R}^{\star n}]_{j_c}|\big)\Big). \end{array}$$

Then, summing over $j_c$, multiplying by $dx_-$ and owing the fact that $L_{11}dx_+, L_{12}dx_-$ are bounded as operators from $L^p$ to $L^p$((Proposition 2), one gets:

$$\|\tilde{S}^{\star n+1}\|^p_{L^p([0,1])} \leq (1+Cdt)^p\big(\|\tilde{S}^{\star n}\|^p_{L^p([0,1])} + dt\|\tilde{R}^{\star n}\|^p_{L^p([0,1])} + C|\tilde{R}^{\star n}_{\alpha N}|^p dx_-\big)$$

where the last term corresponds to the boundary condition at $x = 1$.

Thus, it is possible to take an $\eta > 0$ such that $\mathcal{E}^n := \|\tilde{R}^{\star n}\|^p_{L^p([0,1])} + \eta\|\tilde{S}^{\star n}\|^p_{L^p([0,1])}$ verifies:

$$\mathcal{E}^{n+1} \leq (1+Cdt)^p(\mathcal{E}^n + \|f^n\|^p_{L^p([0,1])}dt)$$

which immediately gives the result of the Lemma by induction. □

Now we are able to prove Lemma 2:

*Proof of Lemma 2.* By using Lemma 1, we have:

$$\|\tilde{\Gamma}_{11}R^n\|_{L^p([0,1])} \leq Cdx_-\|R^n\|_{L^p([0,1])}.$$

By Proposition 2, one can bound $\|R^n\|_{L^p([0,1])}$ by $\|R^{\star n}\|_{L^p([0,1])} + \|S^{\star n}\|_{L^p([0,1])}$ to get:

$$\|\tilde{\Gamma}_{11}R^n\|_{L^p([0,1])} \leq Cdx_-(\|R^{\star n}\|_{L^p([0,1])} + \|S^{\star n}\|_{L^p([0,1])})$$

where we may have changed the constant $C$.

Applying Lemma 3 to $(\tilde{R}^{\star n} - R^{\star n}, \tilde{S}^{\star n} - S^{\star n})_n$, we can conclude easily. This ends the proof of Lemma 2.

□

As a consequence, the energy dynamics of $R^\star, S^\star$ can be estimated by the one of $\tilde{R}^\star, \tilde{S}^\star$. Indeed,

$$\begin{aligned}\|R^{\star n}\|^p_{L^p([0,1])} + \|S^{\star n}\|^p_{L^p([0,1])} \leq\ & C\Big(\|R^{\star n} - \tilde{R}^{\star n}\|^p_{L^p([0,1])} + \|S^{\star n} - \tilde{S}^{\star n}\|^p_{L^p([0,1])} \\ & + \|\tilde{R}^{\star n}\|^p_{L^p([0,1])} + \|\tilde{S}^{\star n}\|^p_{L^p([0,1])}\Big) \\ \leq\ & Cdx^p_- \sum_{m=0}^{n}(\|R^{\star m}\|^p_{L^p([0,1])} + \|S^{\star m}\|^p_{L^p([0,1])})dt \\ & + C\Big(\|\tilde{R}^{\star n}\|^p_{L^p([0,1])} + \|\tilde{S}^{\star n}\|^p_{L^p([0,1])}\Big)\end{aligned}$$

and thus by Grönwall inequality [17, p.1], there exists a constant $C$ independent on the parameters of discretization such that:

$$\begin{aligned}\|R^{\star n}\|^p_{L^p([0,1])} + \|S^{\star n}\|^p_{L^p([0,1])} \leq\ & C\Big(\|\tilde{R}^{\star n}\|^p_{L^p([0,1])} + \|\tilde{S}^{\star n}\|^p_{L^p([0,1])}\Big) \\ & + Cdx^p_- \sum_{m=0}^{n} e^{Cdx^p_-(n-m)dt}(\|\tilde{R}^{\star m}\|^p_{L^p([0,1])} + \|\tilde{S}^{\star m}\|^p_{L^p([0,1])})dt.\end{aligned}$$

Hence for all $T > 0$ fixed and $1 < p < \infty$, there exists a constant $C > 0$ such that:

$$\begin{aligned}\forall ndt \leq T,\ \|R^{\star n}\|_{L^p([0,1])} + \|S^{\star n}\|_{L^p([0,1])} \leq\ & C(\|\tilde{R}^{\star n}\|_{L^p([0,1])} + \|\tilde{S}^{\star n}\|_{L^p([0,1])} \\ & + dx_-\|R^{\star 0}\|_{L^p([0,1])} + \|S^{\star 0}\|_{L^p([0,1])})\end{aligned} \tag{32}$$

where we used Lemma 3 applied to $(\tilde{R}^{\star n}, \tilde{S}^{\star n})_n$.

From now on, we do not make the difference between $R^\star, S^\star$ and $\tilde{R}^\star, \tilde{S}^\star$ keeping the non tilda notation. To prove a finite time stabilization result, the first step is to prove an extinction result for $R^\star$.

**Proposition 3.** *The following estimate holds:*

$$\forall n \geq 0,\ \|R^{\star n}\|_{L^\infty([0,1])} \leq e^{\frac{1}{\sqrt{dt}}(\frac{1}{\lambda_+} - (1-C\sqrt{dt})ndt)}\|R^{\star 0}\|_{L^\infty([0,1])}.$$

*Proof.* We use a Lyapunov argument using the Lyapunov functional firstly introduced in [6] in a continuous setting and then adapted to a discrete framework [14]:

$$V_\gamma(R^{\star n}) := \sup_{1\leq j_f\leq \alpha N} |R^{\star n}_{j_f} e^{-\frac{\gamma}{\lambda_+}x^f_{j_f}}|$$

where $\gamma > 0$ will be chosen later.

Using the scheme verified by $R^\star$ (identified with $\tilde{R}^\star$) (30), it holds for $j_f > 1$:

$$\begin{aligned} |R^{\star n+1}_{j_f} e^{-\frac{\gamma}{\lambda_+}x^f_{j_f}}| \leq & \ (1-\nu_+)|R^{\star n}_{j_f} e^{-\frac{\gamma}{\lambda_+}x^f_{j_f}}| + \nu_+ |R^{\star n}_{j_f-1} e^{-\frac{\gamma}{\lambda_+}x^f_{j_f}}| \\ \leq & \ (1-\nu_+)V_\gamma(R^{\star n}) + \nu_+ e^{-\frac{\gamma}{\lambda_+}dx_+} V_\gamma(R^{\star n}) \\ = & \ (1-\nu_+(1-e^{-\frac{\gamma}{\lambda_+}dx_+}))V_\gamma(R^{\star n}) \end{aligned}$$

and for $j_f = 1$:

$$\begin{aligned} |R^{\star n+1}_{j_f} e^{-\frac{\gamma}{\lambda_+}x^f_{j_f}}| \leq & \ (1-\nu_+)|R^{\star n}_{j_f} e^{-\frac{\gamma}{\lambda_+}x^f_{j_f}}| \\ \leq & \ (1-\nu_+)V_\gamma(R^{\star n}). \end{aligned}$$

As a consequence,

$$V_\gamma(R^{\star n+1}) \leq \ \left(1-\nu_+(1-e^{-\frac{\gamma}{\lambda_+}dx_+})\right) V_\gamma(R^{\star n}).$$

As $e^{-x} \leq 1 - x + \frac{x^2}{2}$ for $x \geq 0$, it holds:

$$V_\gamma(R^{\star n+1}) \leq \left(1-\gamma dt + \frac{1}{2\nu_+}(\gamma dt)^2\right) V_\gamma(R^{\star n}).$$

Owing the fact that $1 + x \leq e^x$, one gets:

$$V_\gamma(R^{\star n+1}) \leq e^{-\gamma dt + \frac{1}{2\nu_+}(\gamma dt)^2} V_\gamma(R^{\star n}).$$

Thus, for $\gamma dt \leq 2\nu_+\varepsilon$ where $\varepsilon$ will be fixed later:

$$\forall n \geq 0,\ V_\gamma(R^{\star n}) \leq e^{-(1-\varepsilon)\gamma n dt} V_\gamma(R^{\star 0}).$$

To finish the proof, we use the fact that:

$$e^{-\frac{\gamma}{\lambda_+}} \| \cdot \|_{L^\infty([0,1])} \leq V_\gamma(\cdot) \leq \| \cdot \|_{L^\infty([0,1])}$$

to conclude that:

$$\forall n \geq 0,\ \|R^{\star n}\|_{L^\infty([0,1])} \leq e^{\gamma(\frac{1}{\lambda_+} - (1-\varepsilon)ndt)} \|R^{\star 0}\|_{L^\infty([0,1])}$$

For $\gamma := 1/\sqrt{dt}$ and $\varepsilon = \frac{1}{2\nu_+}\sqrt{dt}$, we have:

$$\forall n \geq 0,\ \|R^{\star n}\|_{L^\infty([0,1])} \leq e^{\frac{1}{\sqrt{dt}}(\frac{1}{\lambda_+} - (1-\frac{1}{2\nu_+}\sqrt{dt})ndt)} \|R^{\star 0}\|_{L^\infty([0,1])}.$$

This finishes the proof of the proposition. □

A similar analysis for $S^\star$ is given, to deduce the extinction result for all the system.

**Theorem 1.** *For $T > T_{\min}$, there exists a constant $C$ independent on the discretization such that for all $n$ with $\frac{T_{\min}+Cdt^{1/8}}{1-C\sqrt{dt}} \leq ndt \leq$ and for all $(R^{\star 0}, S^{\star 0}) \in L^\infty([0,1])^2$:*

$$\|R^{\star n}\|_{L^\infty([0,1])} + \|S^{\star n}\|_{L^\infty([0,1])} \leq Ce^{-\frac{1}{2dt^{1/8}}}(\|R^{\star 0}\|_{L^\infty([0,1])} + \|S^{\star 0}\|_{L^\infty([0,1])}).$$

*Proof.* By Proposition 3, it holds:

$$\forall ndt \leq T, \|R^{\star n}\|_{L^\infty([0,1])} \leq e^{\frac{1}{\sqrt{dt}}(\frac{1}{\lambda_+}-(1-C\sqrt{dt})ndt)}\|R^{\star 0}\|_{L^\infty([0,1])}. \tag{33}$$

In order to have estimates on $S^\star$, we again proceed by a Lyapunov argument. This time the Lyapunov function is the norm $L^\infty_\gamma$ defined by:

$$\|S^{\star n}\|_{L^\infty_\gamma([0,1])} := \sup_{i_c} |S^{\star n}_{i_c}| e^{\frac{\gamma}{\lambda_-}(x^c_{i_c}-1)}$$

where $\gamma > 0$. Note that in the proof of Proposition 2, we have proven that for $C \leq \gamma \leq \frac{C}{\sqrt{dx_-}}$:

$$\|L_{11}dx_+\|_{\mathcal{L}(L^\infty_\gamma([0,1]))} + \|L_{12}dx_-\|_{\mathcal{L}(L^\infty_\gamma([0,1]))} \leq C$$

**uniformly** in $dt, \gamma$. Then, by similar computations as in the proof of Proposition 3:

$$\begin{aligned}\|S^{\star n+1}\|_{L^\infty_\gamma([0,1])} \leq\ & (1-\nu_-(1-e^{-\frac{\gamma}{\lambda_-}dx_-}))\|S^{\star n}\|_{L^\infty_\gamma([0,1])} + C|R^{\star n}_{\alpha N}| \\ & +(\|L_{11}dx_+\|_{\mathcal{L}(L^\infty_\gamma([0,1]))}\|R^{\star n}\|_{L^\infty_\gamma([0,1])} + \|L_{12}dx_-\|_{\mathcal{L}(L^\infty_\gamma([0,1]))}\|S^{\star n}\|_{L^\infty_\gamma([0,1])})dt.\end{aligned}$$

For $ndt \leq T$,

$$\|S^{\star n+1}\|_{L^\infty_\gamma([0,1])} \leq\ (1-(\gamma-C)dt + C(\gamma dt)^2)\|S^{\star n}\|_{L^\infty_\gamma([0,1])} + C|R^{\star n}_{\alpha N}|.$$

For $\gamma$ such that $C(\frac{1}{\gamma}+\gamma dt) \leq \varepsilon$ ($\varepsilon$ will be fixed later), it holds:

$$\|S^{\star n+1}\|_{L^\infty_\gamma([0,1])} \leq\ e^{-\gamma dt(1-\varepsilon)}\|S^{\star n}\|_{L^\infty_\gamma([0,1])} + Ce^{\frac{1}{\sqrt{dt}}(\frac{1}{\lambda_+}-(1-C\sqrt{dt})ndt)}\|R^{\star 0}\|_{L^\infty([0,1])}.$$

where we have used (33). Let us introduce $n_1 := E\left(\frac{1/\lambda_+ + dt^{1/4}}{dt(1-C\sqrt{dt})}\right)+1$ and for $n_1 \leq n \leq E(T/dt)$, we easily get (by induction):

$$\begin{aligned}\|S^{\star n+1}\|_{L^\infty_\gamma([0,1])} \leq\ & C\|R^{\star 0}\|_{L^\infty([0,1])}\sum_{k=n_1}^n e^{-\gamma(n-k)dt(1-\varepsilon)}e^{\frac{1}{\sqrt{dt}}(\frac{1}{\lambda_+}-(1-C\sqrt{dt})kdt)} \\ & +e^{-\gamma(n-n_1)dt(1-\varepsilon)}\|S^{\star n_1}\|_{L^\infty_\gamma([0,1])} \\ \leq\ & C\|R^{\star 0}\|_{L^\infty([0,1])}e^{-\frac{1}{dt^{1/4}}}\sum_{k=n_1}^n e^{-\gamma(n-k)dt(1-\varepsilon)} + e^{-\gamma(n-n_1)dt(1-\varepsilon)}\|S^{\star n_1}\|_{L^\infty_\gamma([0,1])} \\ \leq\ & \frac{C}{dt}\|R^{\star 0}\|_{L^\infty([0,1])}e^{-\frac{1}{dt^{1/4}}} + e^{-\gamma(n-n_1)dt(1-\varepsilon)}\|S^{\star n_1}\|_{L^\infty_\gamma([0,1])}.\end{aligned}$$

To finish the proof, we use the fact that:

$$e^{-\frac{\gamma}{\lambda_-}}\|\cdot\|_{L^\infty([0,1])} \leq \|\cdot\|_{L^\infty_\gamma([0,1])} \leq \|\cdot\|_{L^\infty([0,1])}$$

to conclude that:

$$\|S^{\star n+1}\|_{L^\infty([0,1])} \leq\ \frac{C}{dt}\|R^{\star 0}\|_{L^\infty([0,1])}e^{\frac{\gamma}{\lambda_-}-\frac{1}{dt^{1/4}}} + e^{\frac{\gamma}{\lambda_-}-\gamma(n-n_1)dt(1-\varepsilon)}\|S^{\star n_1}\|_{L^\infty([0,1])}.$$

For $\gamma = \frac{\lambda_-}{2dt^{1/4}}, \varepsilon = Cdt^{1/4}$, one gets:

$$\|S^{\star n+1}\|_{L^\infty([0,1])} \leq\ \frac{C}{dt}\|R^{\star 0}\|_{L^\infty([0,1])}e^{-\frac{1}{2dt^{1/4}}} + e^{\frac{1}{2dt^{1/4}}-\frac{\lambda_-}{2dt^{1/4}}(n-n_1)dt(1-\tilde{C}\sqrt{dt})}\|S^{\star n_1}\|_{L^\infty([0,1])}.$$

For $ndt \geq \frac{T_{\min}+dt^{1/8}/\lambda_-}{1-\tilde{C}\sqrt{dt}} \iff (n-n_1)dt \geq \frac{1}{1-\tilde{C}\sqrt{dt}} \times (1+dt^{1/8}) \times \frac{1}{\lambda_-}$ :

$$\begin{aligned}\|S^{\star n+1}\|_{L^\infty([0,1])} &\leq \frac{C}{dt}\|R^{\star 0}\|_{L^\infty([0,1])}e^{-\frac{1}{2dt^{1/4}}} + e^{-\frac{1}{2dt^{1/8}}}\|S^{\star n_1}\|_{L^\infty([0,1])} \\ &\leq \frac{C}{dt}\|R^{\star 0}\|_{L^\infty([0,1])}e^{-\frac{1}{2dt^{1/4}}} + Ce^{-\frac{1}{2dt^{1/8}}}\|S^{\star 0}\|_{L^\infty([0,1])}.\end{aligned}$$

Hence,

$$\|S^{\star n+1}\|_{L^\infty([0,1])} \leq Ce^{-\frac{1}{2dt^{1/8}}}(\|R^{\star 0}\|_{L^\infty([0,1])} + \|S^{\star 0}\|_{L^\infty([0,1])}).$$

□

Because of the perturbation term $\tilde{\Gamma}_{11}$ (see also (32)), we lose the convergence in $e^{-\frac{1}{2dt^{1/8}}}$. The final result is given in the next corollary.

**Corollary 1.** *For $T > T_{\min}$ and $1 < p < \infty$, there exists a constant $C$ independent on the discretization such that for all $n$ with $\frac{T_{\min}+Cdt^{1/8}}{1-C\sqrt{dt}} \leq ndt \leq$ and for all $(R^0, S^0) \in L^\infty([0,1])^2$:*

$$\|R^n\|_{L^p([0,1])} + \|S^n\|_{L^p([0,1])} \leq Cdx_-(\|R^0\|_{L^\infty([0,1])} + \|S^0\|_{L^\infty([0,1])}).$$

*Proof.* Immediate from (32), Proposition 2 and Theorem 1. □

# 4 A numerical example

## 4.1 Comparison with the naive method

Here we give a numerical example with $h = 1$, $M_{12} = 2$, $M_{21} = 3$, $\lambda_+ = \lambda_- = 1$, $dt = 1/1000$. For the naive way, we have only one discretization *ie* $\alpha = 1$ for which we take a $CFL = 0.8$. The naive way gives a converged result for the kernel represented in Figure 12.

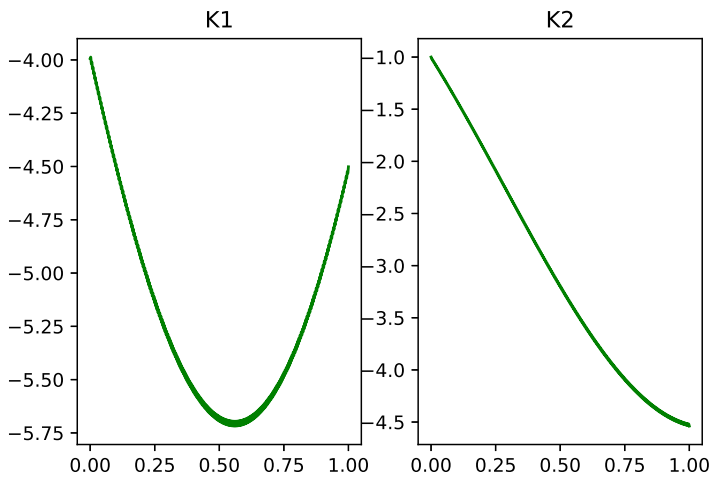


.

Figure 12: The kernels of the closed-loop operator for the naive method

The kernels $K_1, K_2$ represents the functions such that:

$$\forall n, u^n = K_1 R dx_+ + K_2 S dx_-.$$

The spectrum is given in Figure 13.

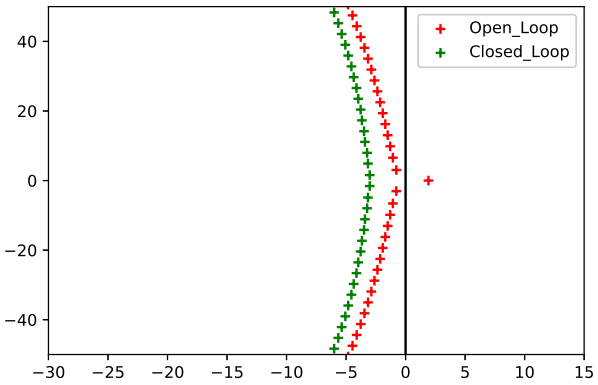


Figure 13: The spectrum of the closed loop operator for the naive method

For our scheme with $\alpha = 2, dt = 1/1000, dx_+ = 1/800, dx_- = 1/400$, the kernels are represented in Figure 14:

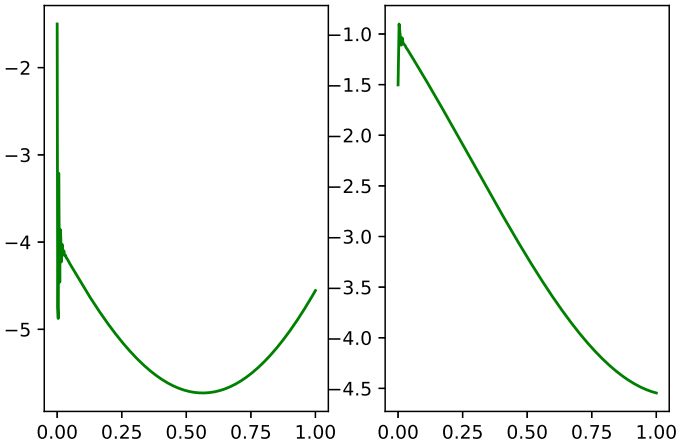


Figure 14: The kernels of the closed-loop operator for less naive method

However, the spectrum of the closed loop system is much closer to its "continuous" equivalent whose spectrum is rejected at infinity. This is displayed in Figure 15.

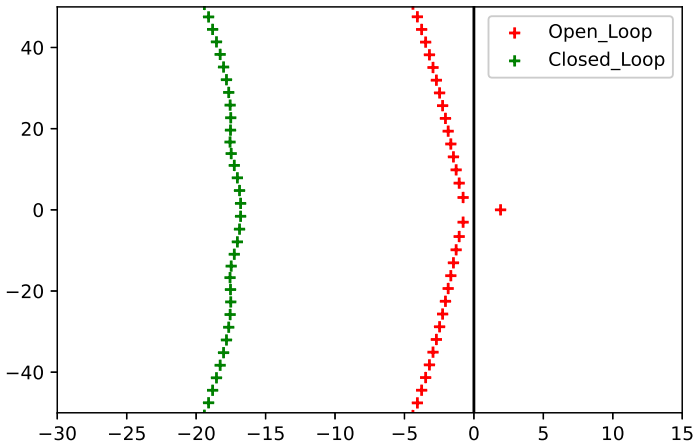


Figure 15: The spectrum of the closed loop operator for the less naive method

Indeed, we have a much stronger rate of convergence for our method than the the naive one. To see this, take an initial data:

$$\begin{cases} R^0(x) &= -4\sin(50x) \\ S^0(x) &= 2 \times \mathbb{1}_{x\leq 0.5} - \cos(50x). \end{cases} \tag{34}$$

and look at the evolution of the $L^2$ norm of the solution as time goes by. The comparison between both methods is shown in Figure 16.

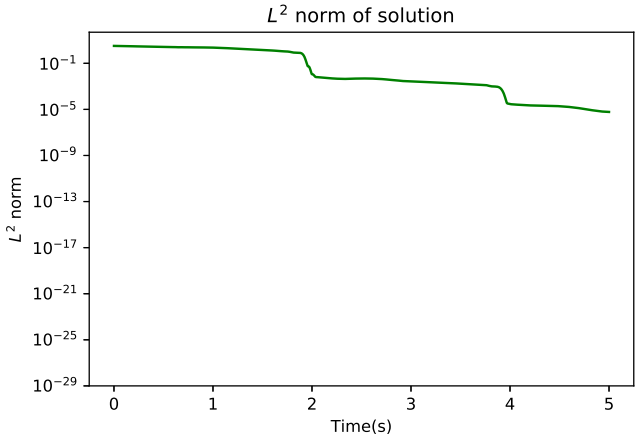


(a) The naive method ($CFL = 0.8$)

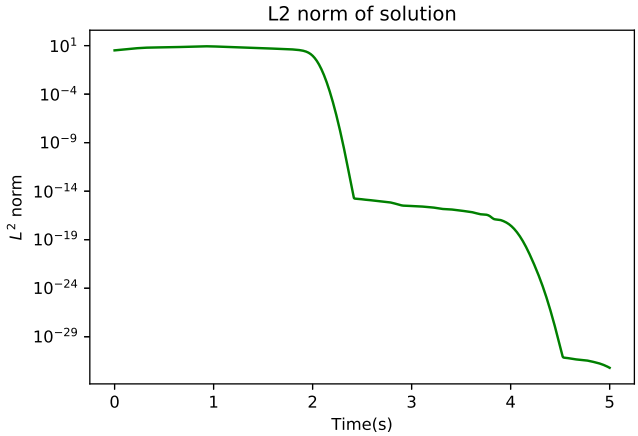


(b) Our method ($\nu_+ = 0.8, \nu_- = 0.4$)

Figure 16: The $L^2$ norm of the solution (log10 scale)

Our method gives much more dissipation than the naive one. This is why it represents better the behaviour of the "continuous" solution which extinguishes at a finite time ($T_f = 2$).

## 4.2 The effect of the perturbation term

In order to observe the effect of the perturbation term $\tilde{\Gamma}_{11}$, we need to take a larger zeroth order term $M$. The parameters are now $h = 1$, $M_{12} = 8$, $M_{21} = -8$, $\lambda_+ = \lambda_- = 1$, $dt = \frac{1}{1000}$, $dx_+ = 1/800, dx_- = 1/200$

($\alpha = 4$) and the initial data is given by (34). The Figure 17 gives energy dynamics:

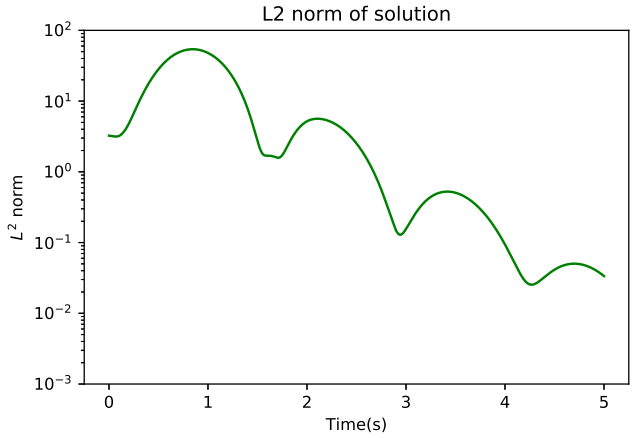


(a) $dt = 1/1000, dx_+ = 1/800, dx_- = 1/200$

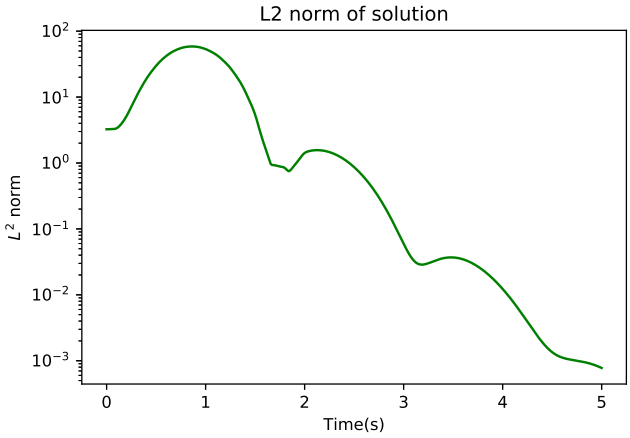


(b) $dt = 1/4000, dx_+ = 1/3200, dx_- = 1/800$

Figure 17: When the perturbation term is non zero

One can observe that we are far from a finite time stabilization picture since after a time $t > T_{\min} = 2$, the solution has still a lot of energy. Moreover, when the discretization is finer (Figure 17-b), the picture shows a stronger decay of the energy but still, one cannot see a clear extinction at $t = T_{\min}$.

In order to explain this, we need to come back to the results of Lemma 2. In fact, when the zeroth order term $M$ is large, the constant $C$ from Lemma 2 may be very large. Besides, we can estimate it heuristically:

$$C \simeq e^{M_{21} T_{\min}} \simeq 10^7.$$

Hence, when $M$ is large, we need to discretize a lot (in this example $dx_-$ should be at least $10^{-7}$) for $(R^\star, S^\star)$ to be close to $(\tilde{R}^\star, \tilde{S}^\star)$.

As a consequence, the effect of the perturbation term $\tilde{\Gamma}_{11}$ can be important if $dx_-$ is not small enough. To confirm this, now take a different discretization for which the perturbation term $\tilde{\Gamma}_{11}$ is zero. After Remark 4, this is the case when the fine grid is two times finer than the coarse one ($\alpha = 2$). Take for example, $dt = 1/1000, dx_+ = 1/800, dx_- = 1/400$ to obtain Figure 18:

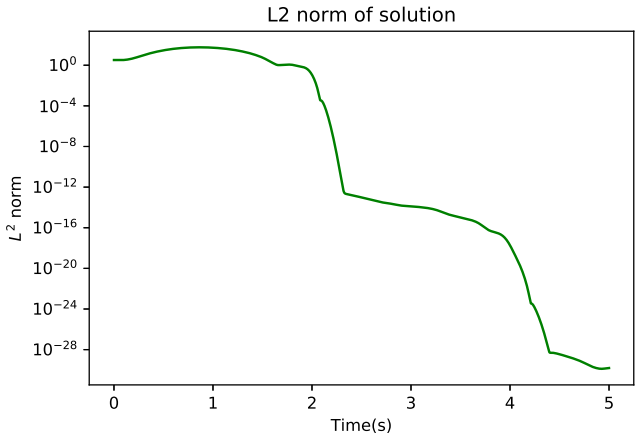


(a) The energy

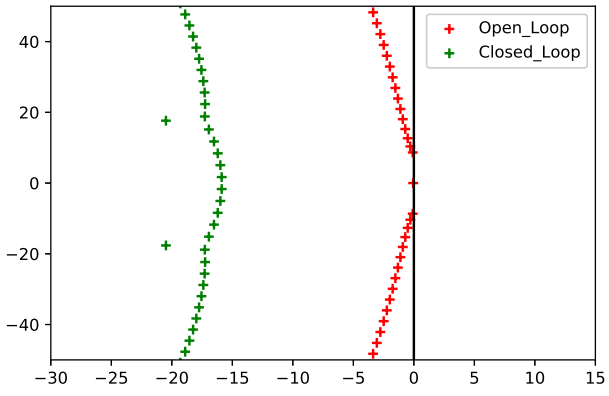


(b) The spectrum

Figure 18: When the perturbation term is zero

Here, the finite time extinction is clear and after $t \simeq T_{\min}$, the solution is of the order of at least $e^{-\frac{1}{2dt^{1/8}}}$ (see Theorem 1).

### 4.3 The case of different velocities

For completeness, we illustrate that our method works for the case were $\lambda_1 \neq \lambda_2$ ,$\alpha > 2$ and when zeroth order term $M$ is moderate. Taking $\lambda_+ = 1$, $\lambda_- = 3$, $M_{12} = 2, M_{21} = 3$, $dt = 1/1000$, $dx_+ = dt$ and $dx_- = 4dx_+$ ($\alpha = 4$), one gets Figure 19:

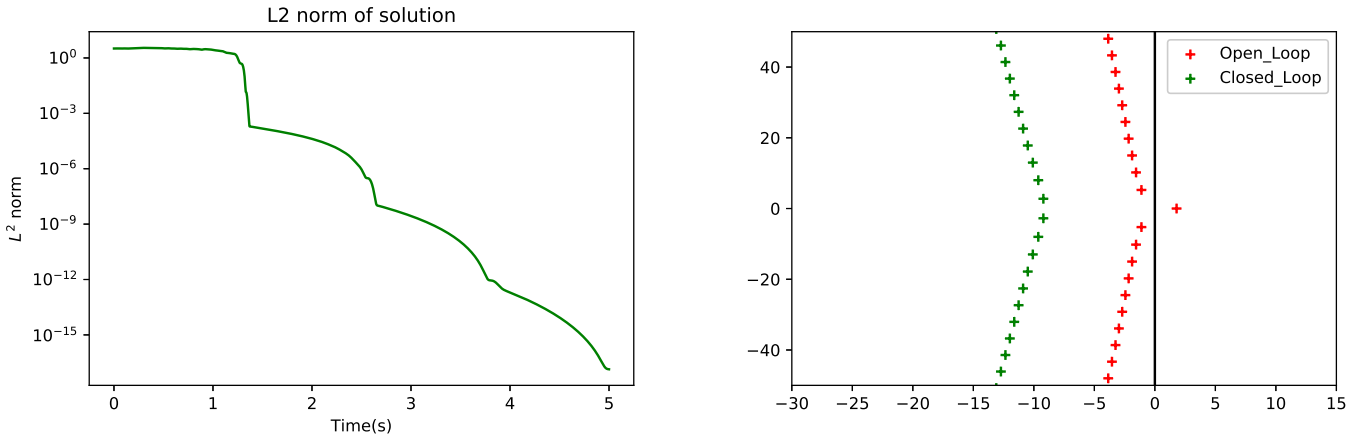


(a) The energy

(b) The spectrum

Figure 19: When velocities are different

## 5 Conclusion

In this paper, it is established that designing a discretized backstepping control must be done with the appropriate scheme. This is why we discretized the system first and then designed a backstepping control adapted to the numerical open-loop system. Doing so, an approximate finite-time stabilization result was shown for the numerical system.

The natural question which comes into play is how can we construct a similar control when the numbers $d_1, d_2$ of equations are larger. We can quote papers [11] where $d_1 = 1$ and $d_2 \in \mathbb{N}^\star$ and [18] where $d_1, d_2 \in \mathbb{N}^\star$ for the continuous theory. In these papers, the authors design a backstepping control to have exponential stabilization. Another interesting question is the influence of the choice of the scheme. Here we took the upwind scheme but it well known that it is very diffusive and gives poor results in simulation. It would be interesting to see if we can extend the numerical backstepping method to higher order schemes like the slope limiter [22] one for example. This is not an easy task since slope limiter schemes are nonlinear even if the PDE system is linear. Finally, it would be interesting to generalize the method to a larger class of grids where the coarse grid is not a subgrid of the fine one.

## References


[1] J. Auriol. *Robust design of backstepping controllers for systems of linear hyperbolic PDEs*. PhD thesis, Mines ParisTech, Paris, 2018.

[2] A. Aw and M. Rascle. Resurrection of "second order" models of traffic flow. *SIAM J. Appl. Math.*, 60(3):916–938, 2000.

[3] G. Bastin and J.-M. Coron. On boundary feedback stabilization of non-uniform linear $2 \times 2$ hyperbolic systems over a bounded interval. *Systems Control Lett.*, 60(11):900–906, 2011.

[4] G. Bastin and J.-M. Coron. *Stability and boundary stabilization of 1-D hyperbolic systems*, volume 88 of *Prog. in Nonlinear Differential Equations and their Applications*. Birkhäuser/Springer, 2016.

[5] G. Bastin, J.-M. Coron, and B. d'Andréa Novel. On Lyapunov stability of linearised Saint-Venant equations for a sloping channel. *Netw. Heterog. Media*, 4(2):177–187, 2009.

[6] J.-M. Coron. On the null asymptotic stabilization of the two-dimensional incompressible Euler equations in a simply connected domain. *SIAM J. Control Optim.*, 37(6):1874–1896, 1999.

[7] J.-M. Coron, R. Vazquez, M. Krstic, and G. Bastin. Local exponential $H^2$ stabilization of a $2 \times 2$ quasilinear hyperbolic system using backstepping. *SIAM J. Control Optim.*, 51(3):2005–2035, 2013.

[8] J. de Halleux, C. Prieur, J.-M. Coron, B. Novel, and G. Bastin. Boundary feedback control in networks of open channels. *Automatica J. IFAC*, 39:1365–1376, 2003.

[9] F. Di Meglio. *Dynamic and control of slugging in oil production*. PhD thesis, Mines ParisTech, Paris, 2011.

[10] F. Di Meglio, G. Kaasa, N. Petit, and V. Alstad. Slugging in multiphase flow as a mixed initial-boundary value problem for a quasilinear hyperbolic system. In *Proceedings of the 2011 American Control Conference*, pages 3589–3596, 2011.

[11] F. Di Meglio, R. Vazquez, and M. Krstic. Stabilization of a system of $n+1$ coupled first-order hyperbolic linear pdes with a single boundary input. *IEEE Transactions on Automatic Control*, 58(12):3097–3111, 2013.

[12] A. Diagne, G. Bastin, and J-M. Coron. Lyapunov exponential stability of 1-D linear hyperbolic systems of balance laws. *Automatica J. IFAC*, 48(1):109–114, 2012.

[13] S. Dudret, K. Beauchard, F. Ammouri, and P. Rouchon. Stability and asymptotic observers of binary distillation processes described by nonlinear convection/diffusion models. In *2012 American Control Conference (ACC)*, pages 3352–3358, 2012.

[14] M. Dus. Exponential stability of a general slope limiter scheme for scalar conservation laws subject to a dissipative boundary condition. Preprint, January 2021.

[15] A. Hayat. Boundary stability of 1-D nonlinear inhomogeneous hyperbolic systems for the $C^1$ norm. *SIAM J. Control Optim.*, 57(6):3603–3638, 2019.

[16] A. Hayat. On boundary stability of inhomogeneous $2 \times 2$ 1-D hyperbolic systems for the $C^1$ norm. *ESAIM Control Optim. Calc. Var.*, 25:31, 2019.

[17] J. M. Holte. Discrete gronwall lemma and applications. Technical report, MAA north central section meeting at und, 2009.

[18] L. Hu, F. Di Meglio, R. Vazquez, and M. Krstic. Control of homodirectional and general heterodirectional linear coupled hyperbolic pdes. *IEEE Transactions on Automatic Control*, 61(11):3301–3314, 2016.

[19] M. Krstic, P. V. Kokotovic, and I. Kanellakopoulos. *Nonlinear and Adaptive Control Design*. John Wiley and Sons, Inc., USA, 1st edition, 1995.

[20] M. Krstic and A. Smyshlyaev. Backstepping boundary control for first-order hyperbolic pdes and application to systems with actuator and sensor delays. *Systems & Control Letters*, 57(9):750 – 758, 2008.

[21] M. Krstic and A. Smyshlyaev. *Boundary control of PDEs*, volume 16 of *Advances in Design and Control*. Society for Industrial and Applied Mathematics (SIAM), Philadelphia, PA, 2008. A course on backstepping designs.

[22] R. J. LeVeque. *Finite volume methods for hyperbolic problems*. Cambridge Texts in Applied Mathematics. Cambridge University Press, Cambridge, 2002.

[23] A. Smyshlyaev, B. Guo, and M. Krstic. Arbitrary decay rate for euler-bernoulli beam by backstepping boundary feedback. *IEEE Transactions on Automatic Control*, 54(5):1134–1140, 2009.

[24] A. Smyshlyaev and M. Krstic. *Adaptive control of parabolic PDEs*. Princeton University Press, Princeton, NJ, 2010.

[25] Xu, C.-Z. and Sallet, G. Exponential stability and transfer functions of processes governed by symmetric hyperbolic systems. *ESAIM Control Optim. Calc. Var.*, 7:421–442, 2002.